

Elsevier required licence: © <2022>. This manuscript version is made available under the CC-BY-NC-ND 4.0 license <http://creativecommons.org/licenses/by-nc-nd/4.0/>
The definitive publisher version is available online at <http://doi.org/10.1016/j.scitotenv.2021.150405>

Spatial modeling of soil erosion hazards and crop diversity change with rainfall variation in the Central Highlands of Sri Lanka

Sumudu Senanayake^{1,2}, Biswajeet Pradhan^{1,3,4*}, Alfredo Huete^{1,5}, Jane Brennan¹

¹ The Centre for Advanced Modelling and Geospatial Information Systems (CAMGIS), Faculty of Engineering and IT, University of Technology Sydney, Sydney, 2007 NSW, Australia

² Natural Resources Management Centre, Department of Agriculture, Peradeniya, 20400, Sri Lanka.

³ Department of Energy and Mineral Resources Engineering, Sejong University, Choongmu-gwan, 209 Neungdong-ro, Gwangjin-gu, Seoul 05006, Korea

⁴ Earth Observation Center, Institute of Climate Change, University Kebangsaan Malaysia, 43600 UKM, Bangi, Selangor, Malaysia

⁵ Faculty of Science, University of Technology Sydney, Sydney, NSW 2007, Australia.

* Correspondence: Biswajeet.Pradhan@uts.edu.au; or biswajeet24@gmail.com

Abstract

The spatial variation of soil erosion is essential for farming system management and resilience development, specifically in the high climate hazard vulnerable tropical countries like Sri Lanka. This study aimed to investigate climate and human-induced soil erosion through spatial modeling. Remote sensing was used for spatial modelling to detect soil erosion, crop diversity, and rainfall variation. The study employed a time-series analysis of several variables such as rainfall, land-use land-cover (LULC) and crop diversity to detect the spatial variability of soil erosion in farming systems. Rain-use efficiency (RUE) and residual trend analysis (RESTREND) combined with a regression approach were applied to partition the soil erosion due to human and climate-induced land degradation. Results showed that soil erosion has increased from 9.08 Mg/ha/yr to 11.08 Mg/ha/yr from 2000 to 2019 in the Central Highlands of Sri Lanka. The average annual rainfall has increased in the western part of the Central Highlands, and soil erosion hazards such as landslides incidence also increased during this period. However, crop diversity has been decreasing in farming systems, namely wet zone low country (WL1a) and wet zone mid-country (WM1a), in the western part of the Central Highlands. The RUE and RESTREND analyses reveal climate-induced soil erosion is responsible for land degradation in these farming systems and is a threat to sustainable food production in the farming systems of the Central Highlands.

32 **Keywords:** Soil erosion; rainfall variation; crop diversity change; remote sensing; GIS; Sri
33 Lanka

34 **1. Introduction**

35 The global (macro and micro) climate variations inevitably influence agricultural food
36 production. Tropical regions are more vulnerable in terms of reducing land productivity due to
37 increasing temperature and monsoon rainfall variation (Borrelli et al., 2017). Scholars
38 continuously struggle to understand the impact of climate change and to find solutions and
39 adaptation measures to meet the growing food demand (Burrell et al., 2017; Panagos and
40 Katsoyiannis, 2019). Lal (2011) emphasized that understanding the impact of climate change,
41 vulnerability, and successful adaptation measures reduces the impact of unexpected events of
42 climate variation. Similarly, modeling soil erosion and land-use change is important for
43 predicting future impacts to take mitigation measures to secure food supply (Lal, 2011;
44 Panagos and Katsoyiannis, 2019).

45 Human-induced climate and land-use changes greatly contribute to land degradation
46 (Sivakumar, 2007; Lal, 2011; Borrelli and Panagos, 2020). As one of the land degradation
47 types, water-related soil erosion in tropical farming systems reduces agricultural productivity
48 and ecosystem services (Han et al., 2020). Irregular and intense precipitation induce water
49 erosion (Puente et al., 2019). The above-ground vegetation cover with its deep root systems
50 helps to reduce the run-off and mass soil movement and ultimately reduces gully erosion and
51 landslides vulnerability (Vannoppen et al., 2015). This is an important point because, as Poesen
52 (2018) points out, water erosion may induce environmental hazards such as gully erosion and
53 landslides in tropical hillslopes.

54 Plant diversity enhances soil water storage capacity, reduces soil erosion, and improves other
55 ecosystem services (Hou et al., 2016; Hunt et al., 2019). Plant diversity refers to the number of
56 different plant species per land area unit and increases with the plant density and plant cover
57 while improving the functional diversity (Wang et al., 2012). Hou et al. (2016) found that
58 increasing plant diversity inhibits soil erosion under heterogeneous vegetation cover. Several
59 other researchers also found that plant diversity has a substantial impact on soil erosion and
60 helps to protect soil erosion (Pohl et al., 2009; Berendse et al., 2015; Liu et al. 2018).

61 In the tropical region, South Asian countries are highly vulnerable to soil erosion due to climate
62 hazards such as drought, floods, and other extreme rainfall events (Lal, 2011). Sri Lanka ranked
63 as the second country on the global climate risk index in 2019 (Eckstein et al., 2019). South
64 Asian monsoonal rainfalls are varied with increasing sea surface temperatures (Ratna et al.,
65 2021). The rainfall variation is emerging as a serious threat to national food production in Sri
66 Lanka. There are major cropping seasons based on the monsoonal rainfall pattern in Sri Lanka.
67 Evidence shows that the major economic crops such as tea and paddies are heavily impacted
68 by these rainfall variations as 66% of total agricultural croplands are under rain-fed only (Esham
69 and Garforth, 2013). A study by Hewawasam and Illangasinghe (2015), showed that rainfall
70 variation heavily contributes to crop productivity losses and soil erosion in Sri Lanka. Further
71 to this, rainfall variation and extreme events significantly increased soil erosion hazards such
72 as gully erosion and landslides (Dang et al., 2019). Thus, the people and their livelihoods are
73 highly vulnerable to the impact of climate change. The farming systems of Sri Lanka,
74 particularly in the Central Highlands, are increasingly vulnerable to the adverse impact of
75 climate change (Esham and Garforth, 2013).

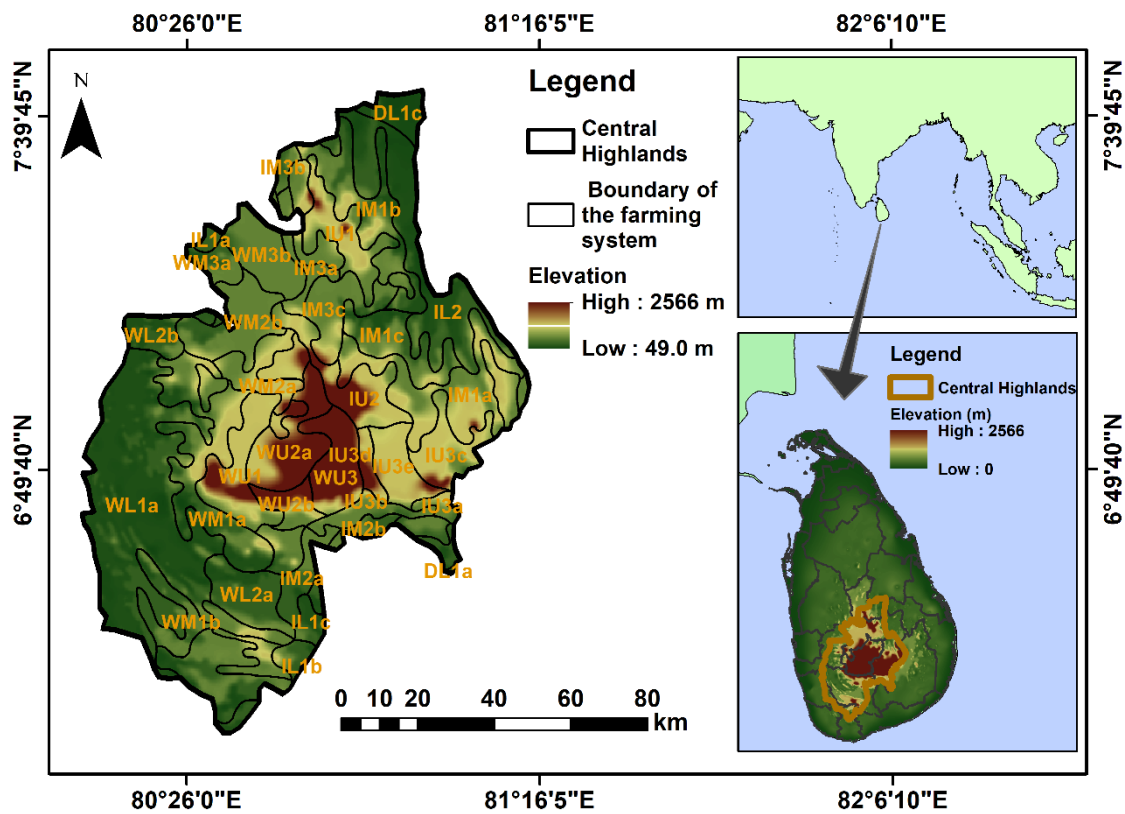
76 Remote sensing data provides useful information to monitor long-term changes in ecosystems
77 and agricultural land management for sustainable food production. Several studies investigated
78 land degradation and plant diversity using various remote sensing technologies with time-series
79 observation (Wessels et al., 2007; Burrell et al., 2017; Mondal et al., 2020). Remote sensing
80 and geographical information system (GIS) have been widely applied to soil erosion and land-
81 use change analysis (Senanayake et al., 2020a; Fenta et al., 2021). However, none of the studies
82 attempted to employ spatial modeling of the soil erosion hazards and plant diversity change
83 with respect to rainfall variation using time-series analysis with geo-informatics tools.
84 Therefore, the specific objectives of this study were set to examine (i) soil erosion hazards and
85 crop diversity changes; and (ii) the relationship between soil erosion hazard and rainfall
86 variation in different farming systems of the Central Highlands in Sri Lanka. The current study
87 provides a novel approach by integrating land-use and land-cover change, soil erosion hazards,
88 crop diversity change and rainfall variation for early detection of soil erosion in the farming
89 systems. This combined spatial modeling approach further enables the partitioning between
90 human and climate-induced land degradation.

91

92

93 **2. Study area**

94 The Central Highlands of Sri Lanka is selected for this study as they are extremely vulnerable
95 to soil erosion hazards, such as landslides and floods (Rathnayake et al., 2020; Ranasinghe et
96 al., 2019). The central region of the country consists of hilly and mountainous terrain
97 (Hewawasam et al., 2013). The total land area is about 10,618 km², and the land rises up to
98 2,500m above sea level. The western side of the region receives much higher rainfall (>2500
99 mm) than the eastern side (2500-1750 mm) (Rathnayake et al., 2020). The region has a high
100 density of landslides distribution. Every year, landslides releases high quantities of sediments
101 to the rivers, especially during the rainy season (Hewawasam, 2010). The Central Highlands
102 has been declared as a protected area by the soil conservation act of Sri Lanka. Figure 1 shows
103 the study area.



104
105
106
107

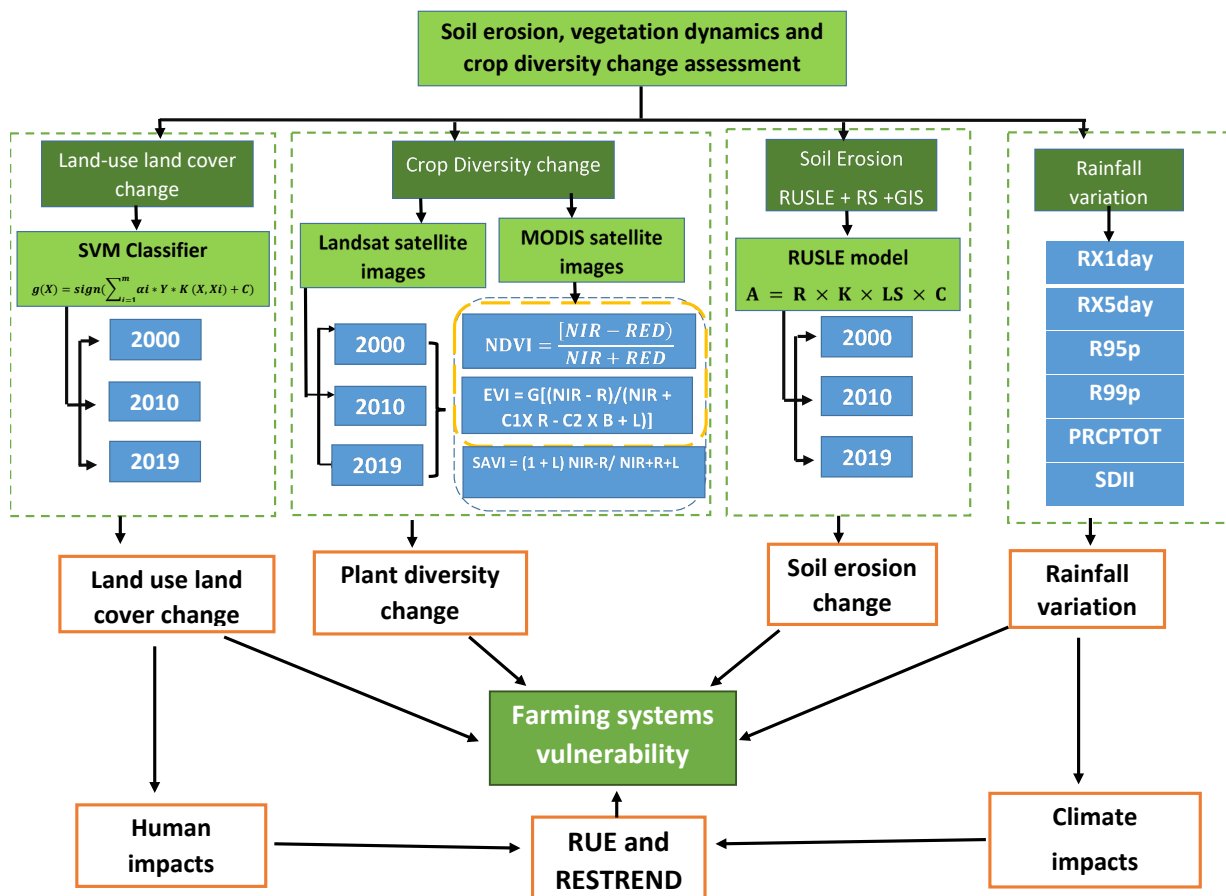
Figure 1. Location of the Central Highlands in Sri Lanka

108 **3. Material and Methods**

109 This study assessed the land-use and land-cover (LULC) change, the spatiotemporal
110 distribution of soil erosion hazards, rainfall variation and crop diversity changes in farming

110 systems of the Central Highlands. The main framework of this study encompassed four major
 111 assessments using spatial modeling techniques. The overall methodology of this study is shown
 112 in Figure 2. The agricultural (cropping) area under each agro-ecological region is considered
 113 as a farming system (Senanayake et al., 2021). There are 34 agro-ecological regions in the
 114 Central Highlands. The primary datasets, including satellite data (Landsat- LT 05, LE 07 and
 115 LC 08), precipitation data (satellite and gauge), topographic data, and landslides incidence from
 116 2000 to 2019, were used in this study. Although Landsat is generally adequate for crop diversity
 117 analysis (Nagendra et al., 2010), cloud cover is one of the major limiting factors for this study
 118 area (Nay et al., 2018) especially to obtain bulk images throughout the year. Hence,
 119 atmospherically-corrected, Moderate Resolution Imaging Spectroradiometer (MODIS)
 120 product data (MOD13Q1) were used for crop diversity analysis. Data sources and spatial
 121 resolution can be found in Appendix A, Table A1 and A2.

122



123

124

125

126

127

Figure 2. The flowchart of the methodology used for this study.

128 **3.1 Land-use and land-cover change analysis**

129 The landuse / landcover (LULC) classification was carried out through the support vector
130 machine algorithm (SVM) using Landsat satellite images (Appendix A, Table A2) from 2000,
131 2010, and 2019. The SVM is a widely used machine-learning method (see Appendix B),
132 introduced by Vladimir Vapnik and co-workers (Cortes and Vapnik, 1995). The Environment
133 for Visualizing Images (ENVI) software was used for image processing. Each acquired image
134 was geometrically corrected and registered into WGS 84 datum and UTM zone 44N projection.
135 The radiometric and atmospheric corrections are prerequisites for generating high-quality
136 images (Chander et al., 2009). The dark object subtraction method was applied to all images
137 (Chavez, 1996) using the ENVI software. LULC time-series analyses were conducted after pan
138 sharpening.

139 The land use maps were developed for 2000, 2010 and 2019. Six land-use classes were
140 identified from the satellite images using land-use maps of the Land Use Policy Planning
141 Department (LUPPD) of Sri Lanka. Olofsson et al. (2013) have highlighted the importance of
142 accuracy assessment: user's, producer's and overall accuracy. Therefore, on average, 7500
143 training pixels were considered for each image to conduct a validation process using a
144 confusion matrix. Finally, Kappa coefficients were derived for each classified image for 2000,
145 2010, and 2019. The Kappa coefficient is commonly used by researchers in accuracy
146 assessment (Qi et al., 2012; Rizeei et al., 2016; Nampak et al., 2018). The Kappa coefficient is
147 given in equation 1 (Bishop et al., 2007).

$$148 \quad Kappa = \frac{N \sum_{i=1}^r X_{ii} - \sum_{i=1}^r (x_{i+})(x_{i+})}{N^2 - \sum_{i=1}^r (x_{i+})(x_{i+})} \quad (1)$$

149
150 where, N is the total number of pixels of the ground truth (Singh et al., 2014) land-use classes,
151 X_{ii} denotes the confusion matrix diagonals, $(x_{i+})(x_{i+})$ are the ground truth pixels in a class
152 and the sum of the classified pixels in that class and the sum of overall classes.

153

154 **3.2 Soil erosion assessment**

155 The soil erosion vulnerability of each farming system in the Central Highlands was derived to
156 find out the pattern of spatial and temporal variation of soil erosion. Although there are several
157 approaches used to estimate soil erosion, a Revised Universal Soil Loss Equation (RUSLE) has
158 been used in this study (see equation 2). The RUSLE method was used due to its easy

159 integration of geo-informatics techniques as well as a practical method of considering a large
160 land area and data-scarce situation. The RUSLE is a widely accepted attractive tool and has
161 been used under different climatic conditions worldwide (Angima et al., 2003; Fernández and
162 Vega, 2018; Alewell et al., 2019). This model has been successfully employed in several
163 applications in tropical counties such as India, Sri Lanka (Ganasri and Ramesh, 2016;
164 Senanayake et al., 2020b), and Malaysia (Nampak et al., 2018).

$$165 \quad A = R \times K \times L \times S \times C \times P \quad (2)$$

166 The annual soil loss per unit area (A) is given in tons per hectare per year. The rainfall erosivity
167 factor (R) ($\text{MJ mm ha}^{-1} \text{ h}^{-1} \text{ yr}^{-1}$) was calculated with rainfall data from the past 30 years (1990-
168 2019). The soil erodibility factor (K) ($\text{t ha h MJ}^{-1} \text{ mm}^{-1}$), slope length and steepness factor (LS)
169 (dimensionless), crop factor (C) (dimensionless) and conservation practices factor (P)
170 (dimensionless) were derived from data gathered from different sources. A detailed description
171 of this analysis is provided in Appendix C. The R , K , LS , C , and P factor layers were computed
172 in 30m gridded raster format. The raster calculator tool in the spatial analysis was used to
173 estimate the annual soil loss in the study area. The final soil erosion raster map was classified
174 into five classes to identify the most vulnerable regions (Senanayake et al., 2020b). The soil
175 erosion hazards maps were generated for 2000, 2010 and 2019.

176 **3.3 Rainfall variation**

177 Rainfall variation was analyzed to provide insight into the impact of climate variation on soil
178 erosion. Rainfall data (ground-based) were collected from five agro-meteorological stations in
179 the Central Highlands (Appendix E, Figure E1). The annual average of rainfall, rainfall
180 anomaly and extreme indices such as maximum 1day precipitation, 95p, 99p (very and
181 extremely wet days), the simple daily intensity index (SDII) and annual total wet day
182 precipitation (PRCPTOT) were computed. Modified Mann-Kandall and Sen's slope tests (see
183 Appendix E, Section E2) were employed to detect significant trends in precipitation indices
184 using the R software for statistical analysis (McLeod and McLeod, 2014).

185 Moreover, the satellite rainfall dataset (PERSIANN-CDR) was downloaded from the Center
186 for Hydrometeorology and Remote Sensing (CHRS) (<https://chrsdata.eng.uci.edu/>). Recent
187 innovative trend analysis test (ITA) developed by Şen (2012), was also employed to evaluate
188 the rainfall trends further (Şen, 2017). Satellite-based PERSIANN-CDR products matched well
189 with the gauge-based precipitation in tropical regions (Sun et al., 2018). The CHRS data were

190 used by many researches due to its capability of assessing rainfall trends(Baez-Villanueva et
191 al., 2018; Sadeghi et al., 2021). A detailed description of this analysis is provided in Appendix
192 E (section E3).

193 **3.3.1 Rainfall variation and soil erosion hazards**

194 Landslides are a good indicator of soil erosion hazards (Pradhan et al., 2012). Landslides
195 inventory (Appendix F, Figure F2) was prepared using the disaster information system of the
196 United Nations International Strategy for Disaster Reduction ‘Desinventar’ (UNISDR, 2021).
197 The relationship between rainfall variation and soil erosion hazards was assessed using the
198 landslides frequency ratio in each farming system. Landslide frequency ratio (FR) for each
199 farming system can be estimated using equation (3) (Lee and Talib, 2005; Meena et al., 2019).

$$200 \quad FR_{(i)} = \frac{S_{(i)}/A_{(i)}}{\sum_1^n (S_{(i)}/A_{(i)})}, \quad (3)$$

201
202 where, S_i the number of pixels containing landslides in class (i), A_i the total number of pixels
203 in class (i).

205 **3.3.2 Rainfall and vegetation indices**

206 The MODIS data (MOD13Q1 - MODIS/Terra Vegetation Indices 16-Day) were downloaded
207 (ORNL DAAC, 2018) from 2000 to 2019 and observed the relationship between NDVI and
208 ground-based and satellite-based rainfall data. Pearson’s correlation coefficient was estimated
209 between these two variables. Linear regression analysis was performed to estimate the
210 coefficient of determination to identify respective trends of the NDVI. The coefficient of
211 determination (R^2) was computed to find how much variability can be caused by its relationship
212 to another related factor (Landmann and Dubovyk, 2014). In addition, the latest modified
213 Kling-Gupta efficiency (KGE’) was used to test the goodness of fit (Appendix I). The results
214 of the parameters were found to be consistent with the Pearson’s correlation coefficient (r),
215 bias (beta), and variability ratio (gamma) (Gupta et al., 2009; Kling et al., 2012).

216 **3.4 Crop diversity change analysis**

217 Estimating plant diversity using remote sensing techniques has been conducted through direct
218 and indirect methods (Turner et al., 2003; John et al., 2008). Direct methods are used with
219 spectral reflectance values and various spatial resolutions from different sensors (Warren et al.,
220 2014). Indirect methods have been derived from environmental parameters or biophysical

221 characteristics, such as primary productivity or habitat structure, which are estimated from
222 remote sensing techniques (Turner et al., 2003; John et al., 2008).

223 Plant diversity has been studied by many researchers using vegetation indices, such as NDVI
224 and EVI (Waring et al., 2006; Levin et al., 2007; Chitale et al., 2019). Several researchers have
225 reported that there is a strong relationship between plant species diversity with vegetation
226 indices such as NDVI (Levin et al., 2007; Pouteau et al., 2018) and the enhanced vegetation
227 index (EVI) (Waring et al., 2006; Morisette et al., 2006). Previous studies indicate that Landsat
228 derived vegetation indices are highly sensitive to plant abundance and species richness in
229 tropical landscapes (Nagendra et al., 2010). Nagendra et al. (2010) found that vegetation
230 indices have low, non-significant relationships with stand density (the number of trees per unit
231 area) and they also found stronger relationships with species richness and diversity. The
232 standard deviation (SD) of the NDVI is positively correlated with total species richness and
233 annual plant richness. Pau et al. (2012) found that NDVI values have increased by 30%- to
234 60% due to variance of tree species richness in a tropical forest (Pau et al., 2012). In addition,
235 they established that NDVI was positively correlated with the tree cover, and NDVI values can
236 be used to distinguish between dense forests and non-forested areas, such as agricultural fields
237 and savannahs. NDVI values range from -1 and $+1$. NDVI values are above zero in vegetated
238 areas and below zero can be assumed to be non-vegetated (Warren et al., 2014).

239 Many investigations have been conducted to identify the relationship associated with the EVI
240 index and plant species richness (Waring et al., 2006; Morisette et al., 2006). There is a positive
241 relationship between EVI and species richness. The EVI is independent of climate drivers
242 (Waring et al., 2006). The EVI was developed to optimize the vegetation signal to improve
243 vegetation monitoring by removing the background soil signal and atmospheric influences
244 (Huete et al., 2002). The difference between the EVI and NDVI of MODIS satellite products
245 is an adjustment for the atmosphere and soil background (Huete et al., 2002). Therefore, it is
246 worth to note that NDVI and EVI can be used for mapping and predicting patterns of species
247 richness in large areas. These applications are relatively low cost (Levin et al., 2007; Nagendra
248 et al., 2010). In addition, researchers commonly use the soil adjusted vegetation index (SAVI)
249 to investigate land degradation. SAVI minimizes the spectral variation caused by the soil
250 background (Huete, 1988). The vegetation indices and the respective equations can be found
251 below (Eq 4-6).

$$\text{NDVI} \qquad \text{NDVI} = \frac{(NIR - RED)}{NIR + RED} \qquad (4) \qquad \text{(Rouse et al., 1974)}$$

SAVI
$$SAVI = \frac{(NIR - RED)(1 + L)}{NIR + RED + L} \quad (5) \quad (\text{Huete, 1988})$$

Where L= correction factor between 0 and 1

EVI
$$EVI = G \frac{(NIR - RED)}{(NIR + C1.RED - C2.B + L)} \quad (6) \quad (\text{Liu and Huete, 1996})$$

G = 2.5; C1 = 6; C2 = 7.5; L = 1

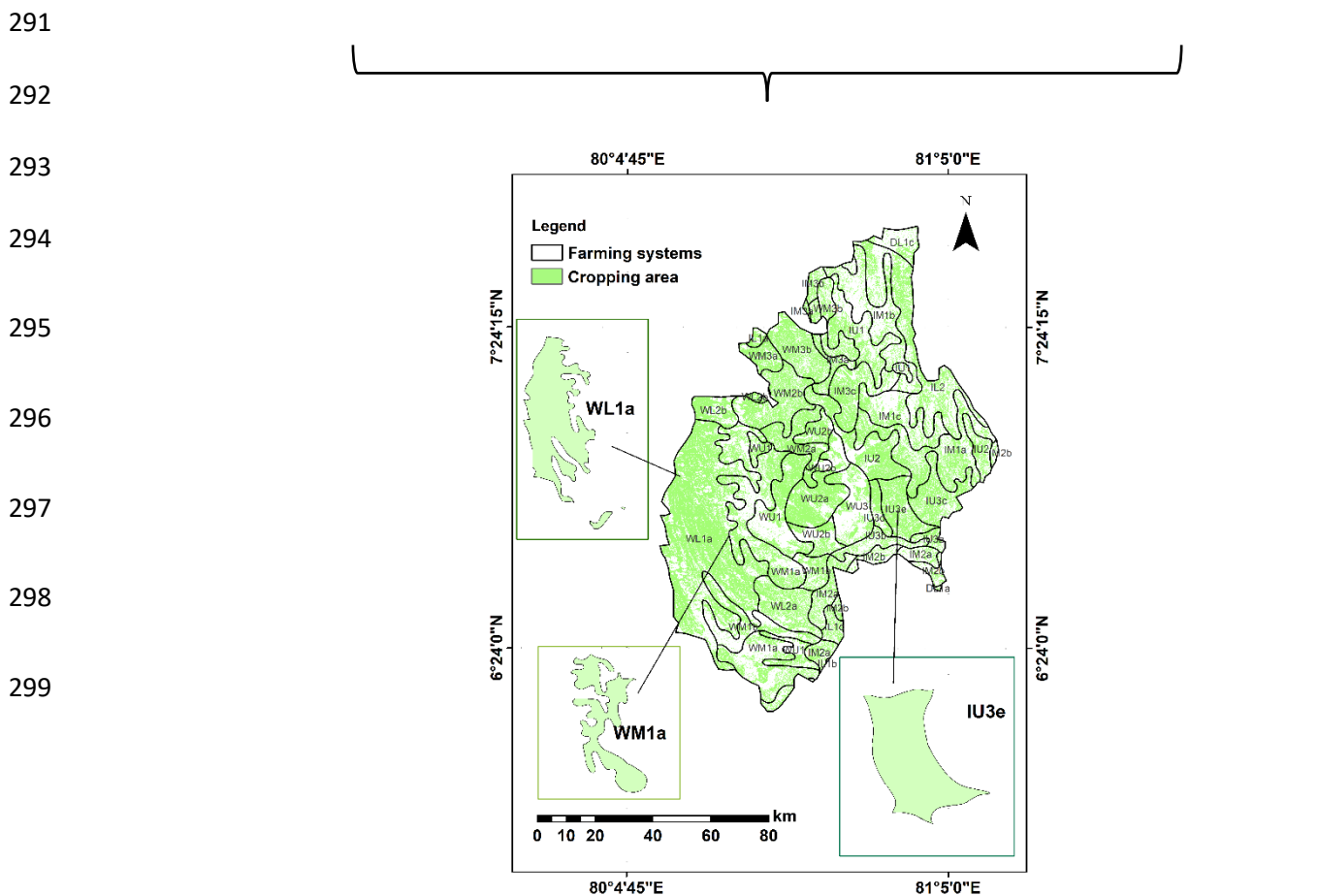
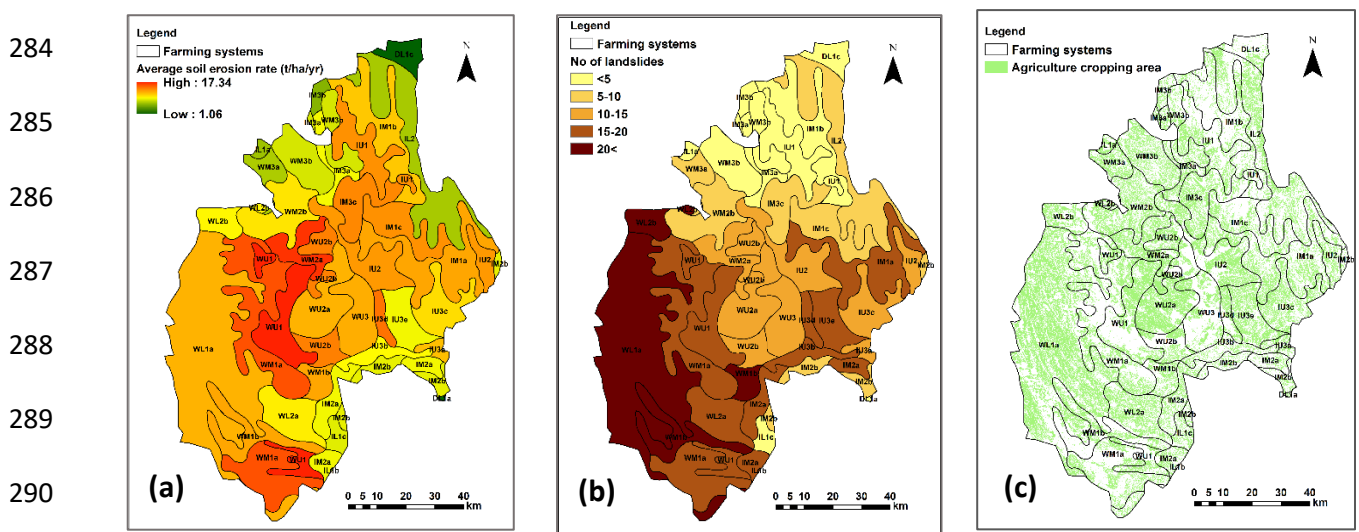
252 This study examines the crop diversity change and soil erosion hazard using NDVI, EVI, and
 253 SAVI using multiple data sources. Yang et al. (2020) highlighted that using various data
 254 sources complements for the cross-validation of a study. Nagendra et al. (2010) claimed that
 255 Landsat imagery is more suitable for vegetation diversity assessment. They found medium-
 256 resolution Landsat ETM+ (30m) correlates stronger than high-resolution IKONOS imagery (4
 257 m) with plant diversity in a dry tropical forest. Due to higher cloud cover around Sri Lanka
 258 throughout the year, trend analysis could not be carried out only with Landsat imageries.
 259 Hence, MODIS -250m 16 days' products (MODIS-MOD13Q1) were used for time series
 260 analysis for the years 2001–2019 (LPDAAC, 2021). The MODIS-derived variables have also
 261 shown the ability to predict plant species richness at the regional level (John et al., 2008). In
 262 addition, MODIS productivity estimates (NDVI/EVI/GPP) are readily available online and
 263 provide global coverage (Huete et al., 2002). The MODIS vegetation index products are
 264 generated by compositing daily data every 16 days, resulting in 23 composites per year and
 265 avoid cloud cover and other effects (Huete et al., 2002).

266 The Shannon diversity index is used to measure plant diversity (Nagendra, 2002). This
 267 diversity index produces an evaluation of landscape richness and evenness. It measures the
 268 number and the relative abundance or evenness of each species. A MODIS derived Shannon
 269 diversity index was used to evaluate the crop diversity during this period. The Shannon
 270 diversity index (SHDI) (Shannon, 1948) is given in equation (7).

271
$$SHDI = 1 - \sum_{i=1}^N P_i \times \ln P_i \quad (7)$$

272 where, N is the number of land cover types, and P_i is the proportional abundance of the i^{th} type
 273 (Nagendra, 2002). This index ranges in theory from 0 to infinity.
 274

275 In this study, crop diversity changes were further assessed using the case study approach. Three
 276 case studies were conducted covering the Central Highlands to identify the crop diversity
 277 changes at the farming system level. The most vulnerable two farming systems (WL1a, WM1a)
 278 and moderate vulnerable farming system (IU3e) for soil erosion were identified based on the
 279 cropping area, soil erosion and number of landslides occurrence in the last two decades. The
 280 following criteria were used to select farming systems for the case studies (Appendix F, Figure
 281 F3): (i) the percentage of land area under high and very high soil erosion hazard classes;
 282 the number of landslides occurrence in the past two decades; and (iii) the agricultural area's
 283 vulnerability to soil erosion. The identified farming systems are given in Figure 3.



300 **Figure 3.** a) Average soil erosion rate, b) the number of landslides occurred, c) agricultural
301 cropping area in the farming system, and d) selected farming systems for three case studies.

302 The Pearson's correlation coefficients (r) were computed to explore the relationship between
303 vegetation indices values, plant species richness and diversity of disturbance types (Warren et
304 al., 2014). Pearson's correlation coefficient provides correlation statistically as a measure of
305 the strength of the linear relationships. Values that are closer to one indicate a stronger
306 relationship or correlation. Statistical models were developed using the linear regression
307 technique.

308

309 **2.4.1 Vegetation indices and soil erosion**

310 Many researchers have used vegetation indices to differentiate soil erosion/land degradation
311 from climate change and anthropogenic activities. The Rain-use efficiency (RUE) and residual
312 trend (RESTREND) indices are derived from vegetation indices (NDVI and EVI) to study land
313 degradation (Wessels et al., 2012; Cunha et al., 2020). RUE and RESTREND analyses have
314 been popularized for assessing the long-term changes in vegetation over the last few decades
315 (Kundu et al., 2017). The following rule of thumb is applied: where vegetation dynamics are
316 strongly driven by rainfall, declining RUE is correlated with land degradation. In humid areas,
317 where vegetation is not as strongly driven by rainfall variation, the NDVI is strongly correlated
318 with vegetation dynamics and may be taken as a proxy for land degradation (Yengoh et al.,
319 2014).

320 **2.4.2 Rain-use efficiency**

321 Rain-use efficiency (RUE) can be used to normalize the effects of rainfall in vegetation
322 productivity (Fensholt et al., 2013; Liu et al., 2015). The RUE is the ratio between the annual
323 sum of vegetation productivity and annual rainfall (Wessels et al., 2012). Temporal change of
324 RUE has been used to detect land degradation (Liu et al., 2015). Prince et al. (1998) highlighted
325 that decreased RUE referred to land degradation by reduced vegetation coverage and increased
326 run-off. The declining RUE is correlated with land degradation (Yengoh et al., 2014). RUE
327 may vary with species distribution (Fensholt et al., 2013). However, some researchers still
328 argue whether RUE is an effective indicator of land degradation (Wessels et al., 2007). The
329 RUE can be derived from equation 8,

$$330 \quad \text{RUE} = \frac{\sum \text{NDVI}}{\text{Average annual rainfall}} \quad (8)$$

331 where, $\sum \text{NDVI}$ is the average annual sum of NDVI.

332 **2.4.3 Residual trend analysis**

333 Residual trend analysis (RESTREND) was proposed by Evans and Geerken (2004). Predicted
334 NDVI indicates the climatic impact on NDVI, whereas observed NDVI is the result of both
335 climate and anthropogenic factors. A negative RESTREND indicates human-induced
336 degradation of vegetation, and a positive RESTREND indicates the improvement of vegetation
337 conditions (Kundu et al., 2017). RESTREND is obtained from the differences between the
338 observed \sum NDVI and the \sum NDVI predicted by the rainfall using regressions calculated for
339 each pixel. The equation for RESTREND is in equation 9 (Wessels et al., 2008; Wessels et al.,
340 2012).

$$341 \quad \text{RESTREND} = \text{observed } \sum \text{NDVI} - \text{predicted } \sum \text{NDVI} \quad (9)$$

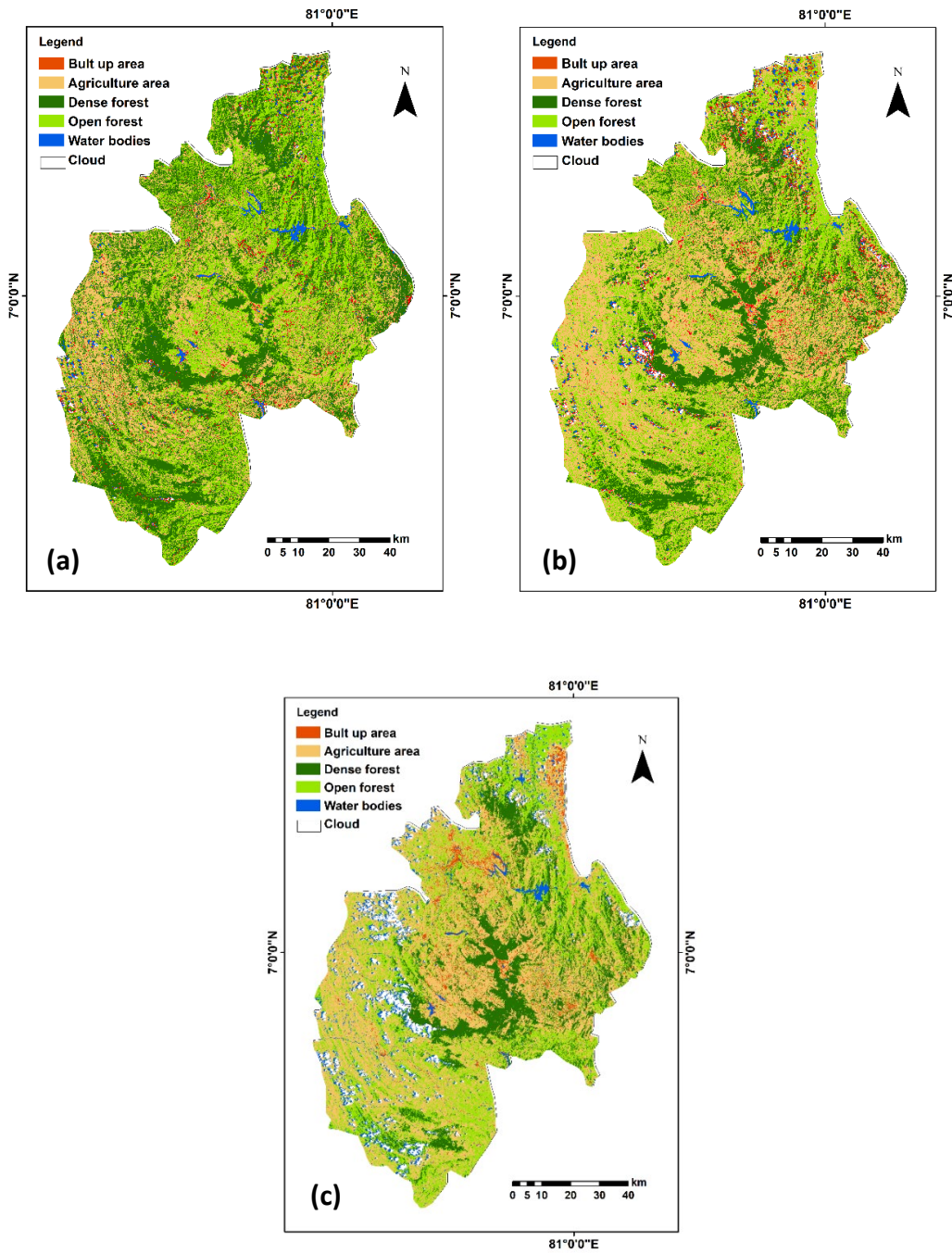
342 In this study, the RUE and RESTREND were employed using NDVI and EVI indices of
343 MODIS data to find the impact of climate and human-induced soil erosion/land degradation.
344 The time-series analysis of NDVI and EVI indices from 2000 to 2019 were used to derive RUE
345 and RESTREND.

346

347 **4. Results**

348 **4.1 Land-use and land-cover change**

349 Land-use and land-cover (LULC) change analysis was carried out using Landsat imagery for
350 2000, 2010 and 2019 by employing the support vector classifier algorithm. The accuracy
351 assessments indicate the Kappa coefficients: 0.83 in 2000, 0.81 in 2010 and 0.83 in 2019 (see
352 Appendix D, Table D2- 4). Figure 4 shows the resulted classification maps for 2000, 2010 and
353 2019. Table 1 shows the respective findings of the analysis. The results indicate that dense
354 forest and open forest have decreased during this period by 14.5% and 5.8%, respectively,
355 while agricultural areas and built-up areas have increased by 15.4% and 2.35%.



356

357

358 **Figure 4.** LULC maps in the Central Highlands: a) 2000, b) 2010, and c) 2019

359

360

361

362

363

364

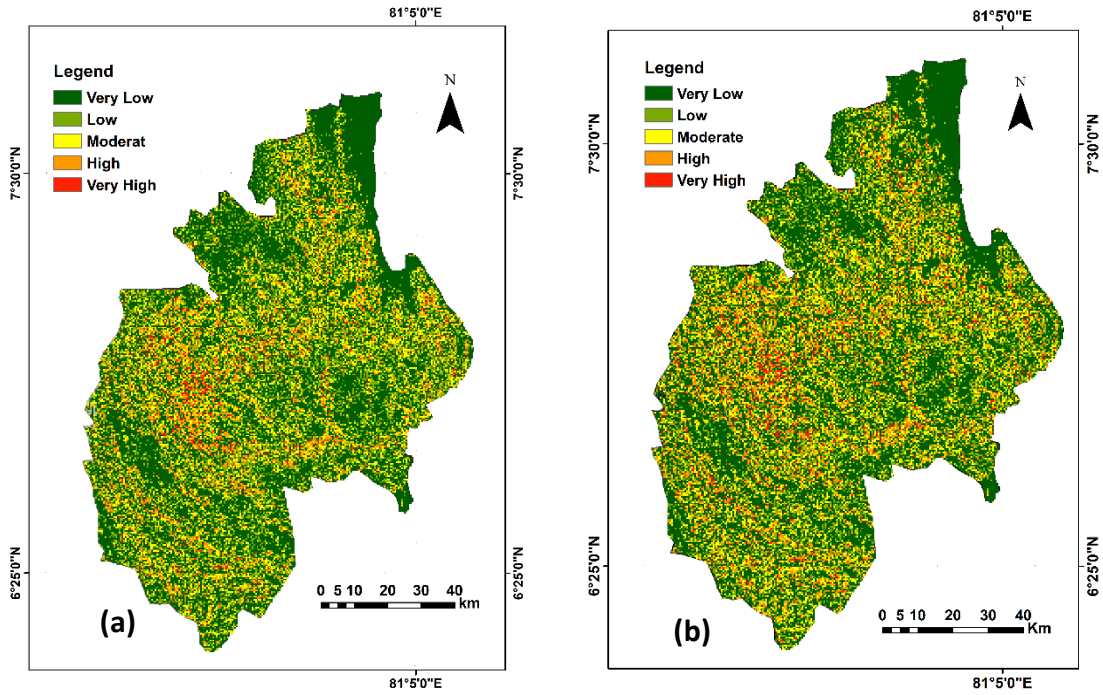
365 **Table 1.** LULC change from 2000 to 2019

Classes	Area (km ²)						Change
	2000	%	2010	%	2019	%	
Dense Forest	3452.9	32.9	2491.9	23.7	1927.5	18.4	-1525.4
Open forest	3761.4	35.8	3391.6	32.3	3150.9	30.0	-610.6
Agriculture area	2718.3	25.9	3881.4	37.0	4333.2	41.3	1614.9
Built-up area	299.5	2.85	373.6	3.6	546.0	5.2	246.5
Water bodies	137.4	1.31	59.9	0.6	137.3	1.3	-0.1
Other (Cloud)	130.4	1.24	383.6	3.7	404.6	3.9	274.2
	10500.0	100.0	10500.0	100.0	10500.0	100.0	

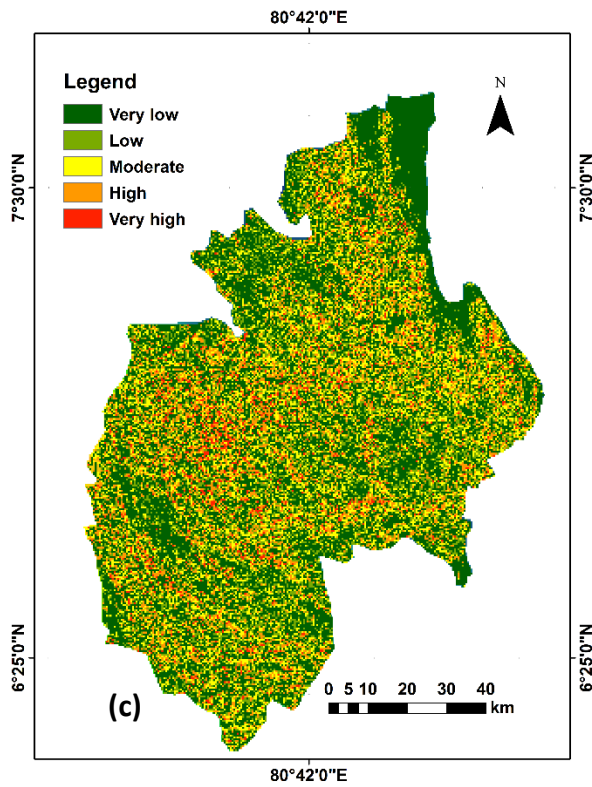
366

367 **4.2 Soil erosion hazards**

368 The generated soil erosion hazards maps are illustrated in figure 5. The details of soil erosion
 369 hazard class distribution from 2000 to 2019 are given in Table 2 and Appendix C (Figure C3).
 370 According to the results of the study, soil erosion rates are increasing. The mean annual soil
 371 erosion rate was 9.08 Mg/ha/yr in 2000, and it increased to 10.17 Mg/ha/yr in 2010 and 11.08
 372 Mg/ha/yr in 2019 (Table 2). The land areas under high and very high soil erosion classes were
 373 increased by 286.1km² and 166.3 km², respectively. The average soil erosion rate and landslide
 374 frequency ratio for each farming system were also assessed. The results are given in Appendix
 375 F, Table F1. The highest soil erosion rates can be observed in farming systems in the wet zone.
 376 This increasing soil erosion trend may be a result of the climate variation and anthropogenic
 377 impact of LULC change.



378



379

380

Figure 5. Soil erosion hazard map for: a) 2000, b) 2010, and c) 2019

381

382

383

384 **Table 2.** The details of soil erosion hazard classes, rates, and area distribution

Class	Soil erosion rate	Area (km ²)			Change
		2000	2010	2019	2000 -2019
Verylow	<5	5494.7	5345.6	5140.3	-354.4
Low	5-10	1733.3	1569.5	1555.3	-178.1
Moderate	10-20	1831.1	1847.4	1911.2	80.2
High	20-50	1221.2	1404.3	1507.3	286.1
Very high	50<	219.7	333.2	385.9	166.3
Total land		10500.0	10500.0	10500.0	
Average annual soil erosion (t/ha/yr)		9.08	10.17	11.08	

385

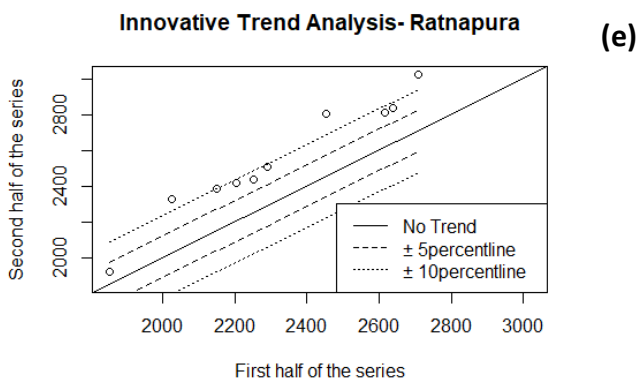
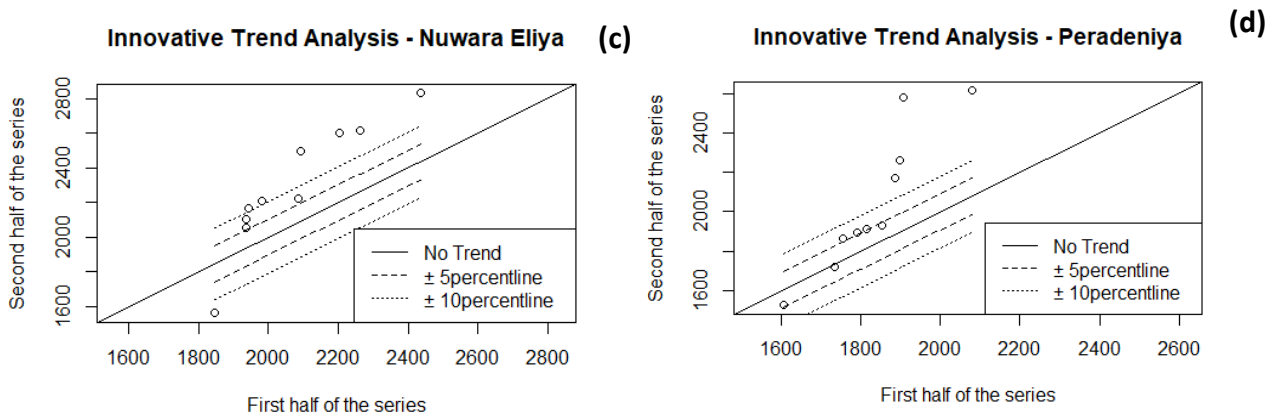
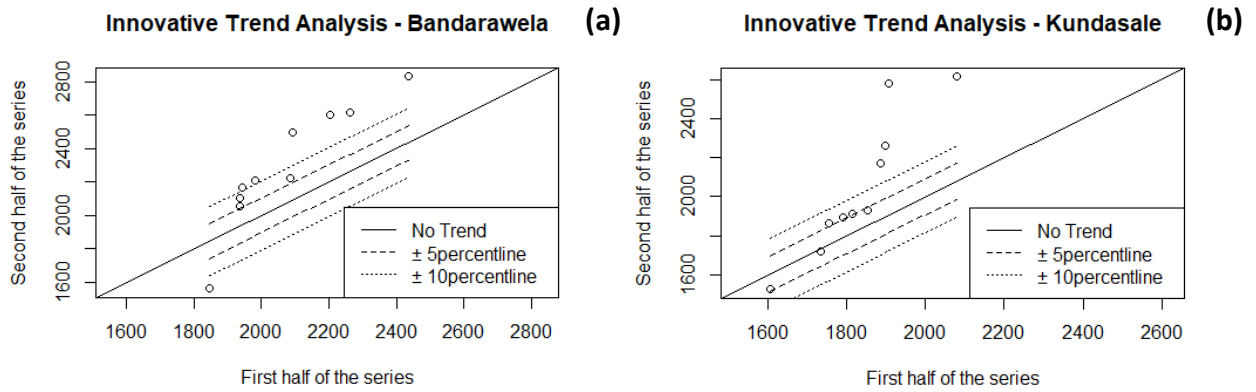
386 **4.3 Rainfall variation**

387 The increasing trend of average annual rainfall could be observed in all stations in the Central
 388 Highlands. According to table 3, satellite-based rainfall data show a significantly increasing
 389 trend in all the stations. Similarly, ground-based rainfall data also indicate significantly
 390 increasing rainfall except in Nuwara Eliya and Kundasale stations. Figure 6 illustrates the
 391 results of innovative trend analysis based on satellite rainfall data. Researchers have reported
 392 the increasing trend of average annual precipitation in Sri Lanka. Nearly 75% of meteorological
 393 stations have shown a significantly increasing trend (Jayawardena et al., 2018).

Table 3. Results for innovative trend test (slope *s*) of annual rainfall in the Central Highlands.

Station	Slope (s)	Trend indicate (r)	Standard deviation (σ)	Slope standard deviation (σs)			Level 99% Sig.	Type of trend
				Level 90% Sig.	Level 95% Sig.	Level 99% Sig.		
Satellite rainfall data								
Ratnapura	22.66**	0.98	317.45	1.61	±2.64	±3.14	±8.17	Increasing
Peradeniya	21.53**	1.18	281.64	2.48	±4.08	±4.86	±6.39	Increasing
Nuwaea Eliya	21.30**	1.03	300.21	2.68	±4.4	±5.24	±5.29	Increasing
Bandarawella	21.30**	1.03	300.21	2.68	±4.40	±5.24	±6.89	Increasing
Kundasale	21.53**	1.18	281.64	2.48	±4.08	±4.86	±6.39	Increasing
Ground-based rainfall data								
Ratnapura	35.53**	0.99	536.89	4.90	±8.60	±9.06	±12.62	Increasing
Peradeniya	22.90**	1.20	381.54	2.71	±4.46	±5.31	±6.99	Increasing
Nuwaea Eliya	3.40	0.20	381.89	3.99	±6.57	±7.83	±10.29	Increasing
Bandarawella	16.97**	1.02	310.07	4.77	±7.84	±9.35	±12.28	Increasing
Kundasale	5.20	0.36	343.97	3.17	±5.22	±6.22	±8.17	Increasing

* and ** represent 95% and 99% significance levels, respectively



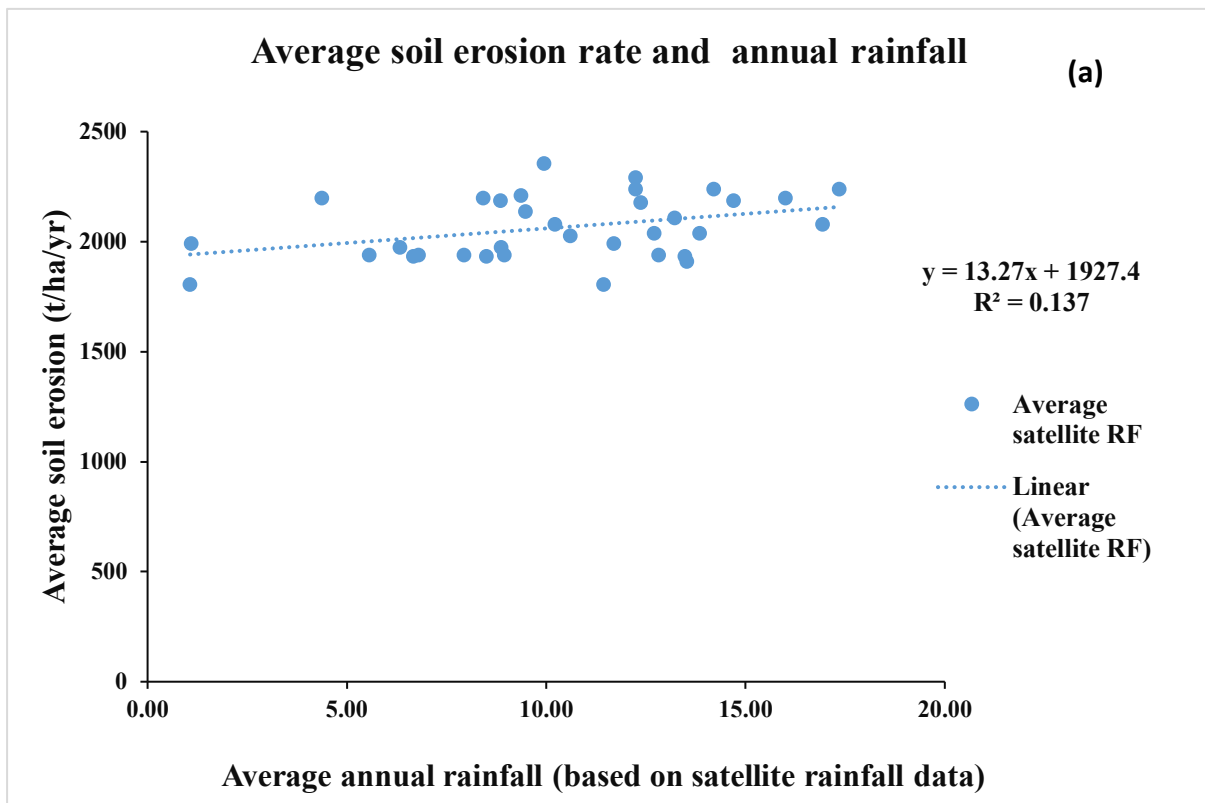
398 **Figure 6.** The Inovative trend analysis in (a) Bandarawela (b) Kundasale, (c) Nuwara Eliya
399 (d) Peradeniya and (e)Ratnapura, stations from satellite-based rainfall data.

400 **4.3.1 The relationship between rainfall variation and soil erosion hazards**

401 Findings indicate that there are positive correlations between variables (Appendix I, Table I1):
402 average annual rainfall and soil erosion rates $r = 0.390$ ($p < 0.05$), landslides frequency ratio and
403 average soil erosion rate $r = 0.416$ ($p < 0.05$). The regression model in Figure 7 shows the

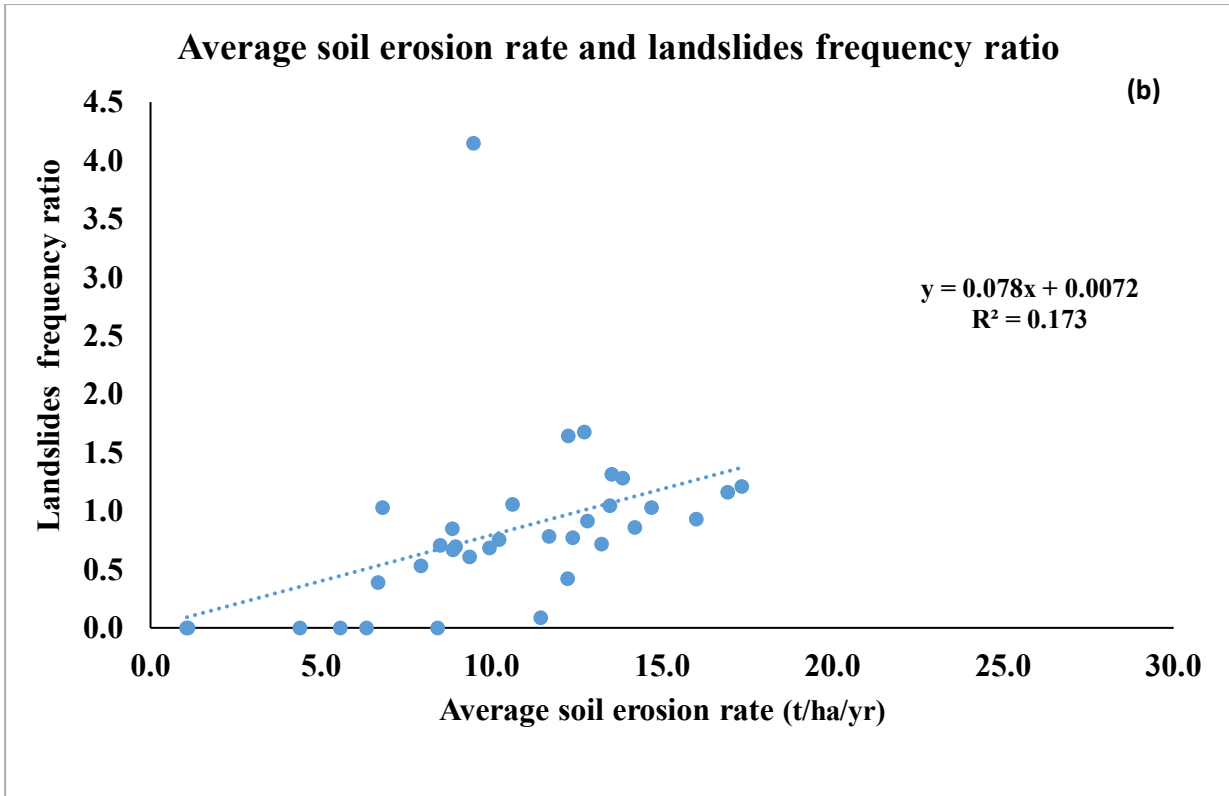
404 relationships between soil erosion rate and average annual rainfall and average soil erosion rate
 405 and landslide frequency ratio in each farming system. Modified Kling–Gupta efficiency values
 406 are shown in table I2. Ranasinghe et al. (2019) highlighted that heavy and prolonged rainfalls
 407 are the main triggering factors for landslides in Sri Lanka. Rozos et al. (2013) argue that soil
 408 erosion could trigger landslides manifestation. Hence, the results of this study indicate that
 409 rainfall erosivity and soil erosion triggers the incidence of landslides in the Central Highlands.
 410 Hence, the results of this study indicate that rainfall erosivity and soil erosion triggers the
 411 incidence of landslides in the Central Highlands.

412

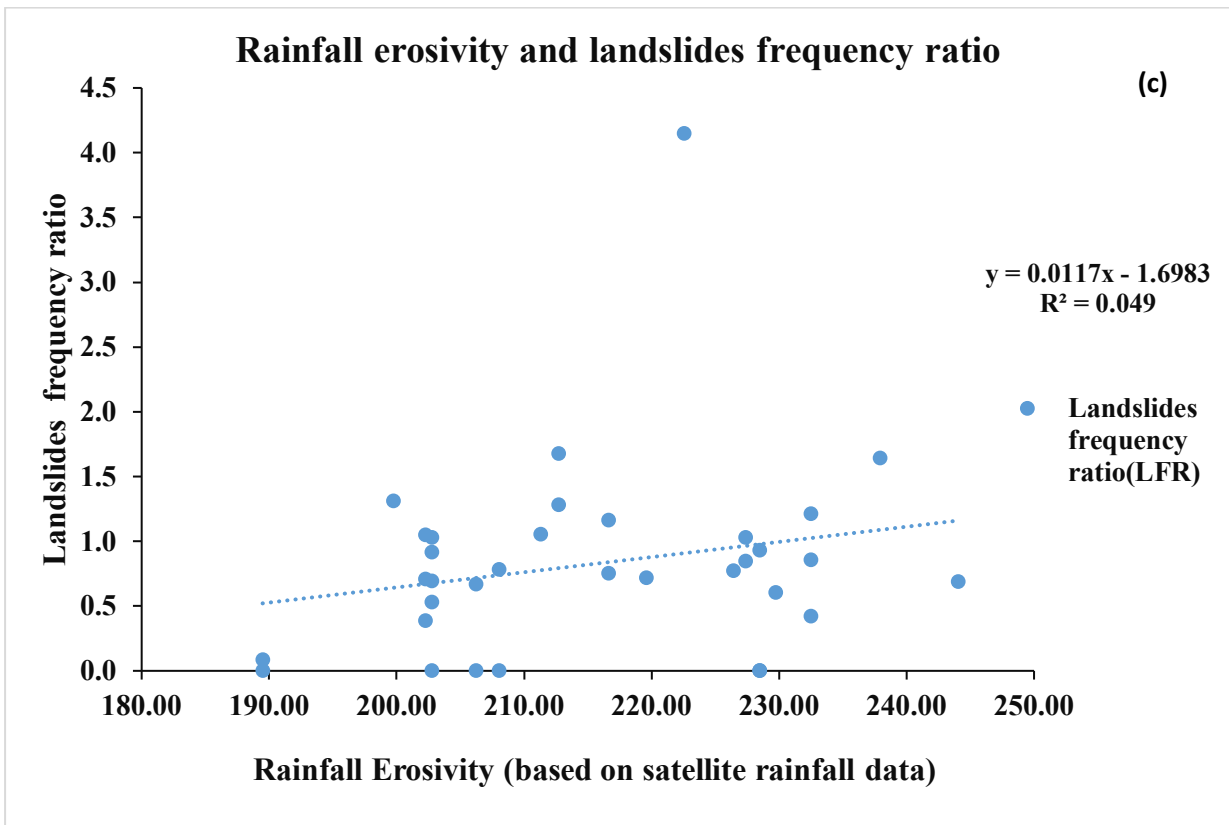


413

414



415



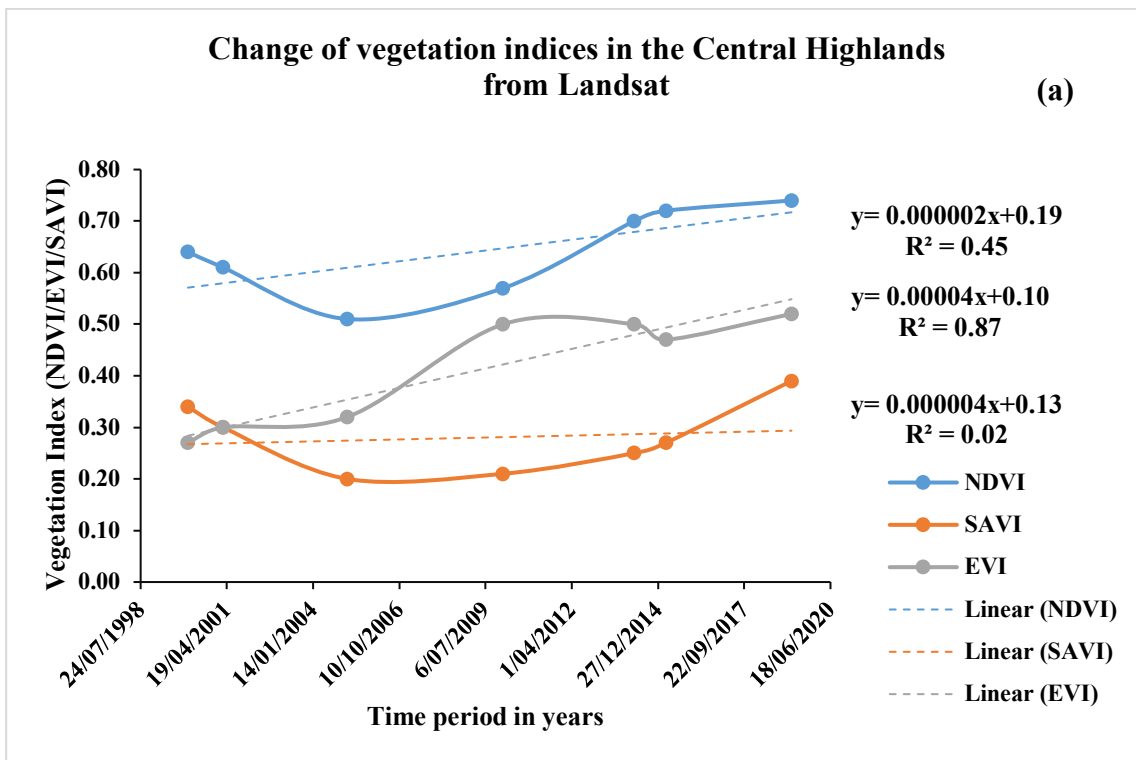
416

417 **Figure 7.** The details of the relationship between a) soil erosion and average annual rainfall
 418 b) average annual soil erosion rate and landslide frequency and (c) rainfall erosivity and
 419 landslides frequency ratio in each farming systems.

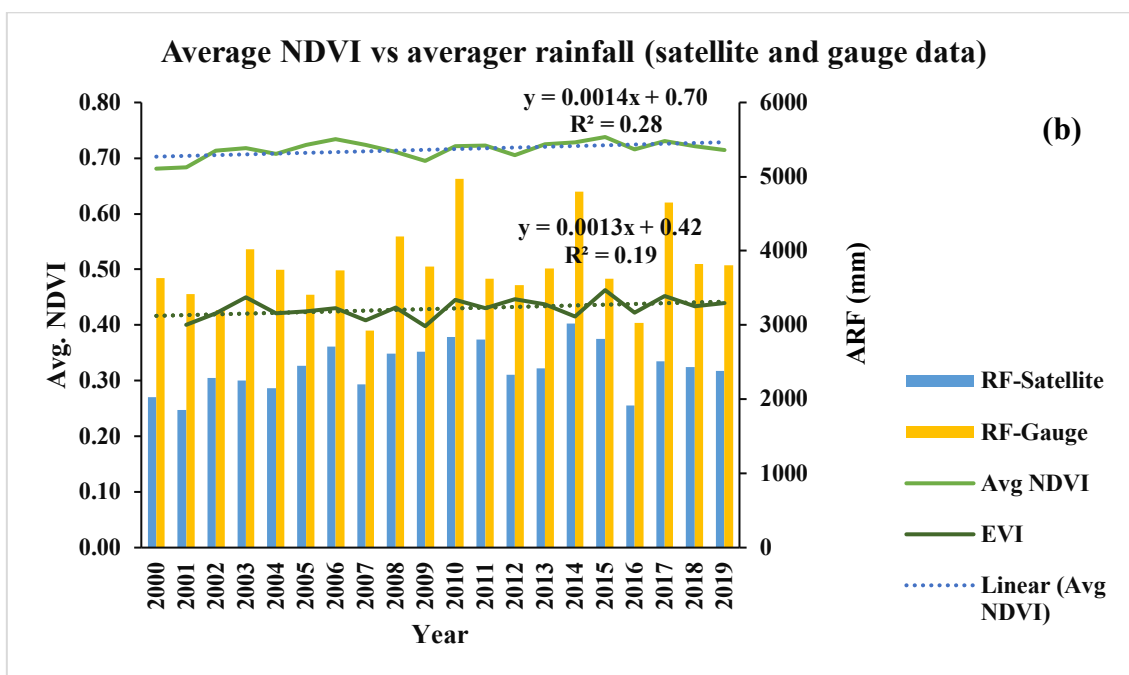
420

421 **4.4 Crop diversity change in the farming systems**

422 Based on the results of vegetation indices, the NDVI, EVI and SAVI show an overall increasing
 423 trend over the years. Figure 8 shows the distribution of vegetation indices over the period and
 424 respective images (Appendix G, Figure G1-3) derived from Landsat and MODIS imagery for
 425 the NDVI, EVI and SAVI.



426



427

428 **Figure 8.** (a) Landsat-derived: NDVI, EVI and SAVI distribution over the period in the
429 Central Highlands and (b) MODIS-derived: NDVI and EVI distribution over the period with
430 annual average rainfall (ARF- satellite and gauge) in Ratnapura area (WL1a).

431 In this research, Landsat data provide the NDVI, EVI and SAVI values that demonstrate the
432 combined effect of land-uses in the Central Highlands: dense forest, open forest, agriculture,
433 water bodies and urban/built-up areas. For further analysis of crop diversity in farming systems,
434 three case studies were conducted. From the analysis of three case studies, a similar pattern of
435 NDVI, and EVI variation could be observed over the years (Appendix H, Figure H1-4). Further
436 to this, the increasing trend of NDVI and EVI was greater than SAVI. Researchers also
437 observed similar trends in other regions (Sarmah et al., 2018; Liu et al., 2018). NDVI is closely
438 related to the net and gross primary productivity. NDVI strongly correlates with plant biomass
439 and net primary productivity (NPP), which is the difference between carbon fixed by
440 photosynthesis and carbon lost to autotrophic respiration (Evans and Geerken, 2004). The
441 MODIS-derived GPP and EVI provide reasonable estimates of productivity in the forest and
442 grassland biomes (Waring et al., 2006). The MODIS derived NDVI and EVI values are
443 positively correlated with NPP (0.76 and 0.53).

444 Earlier researchers have revealed a positive relationship between species richness and
445 productivity (Fensholt et al., 2013), although the relationship may differ among ecosystems
446 and dependent on spatial scales. Therefore, increasing trends in vegetation indices may indicate
447 increasing heterogeneity or species diversity. Hence, this study further analyzed crop diversity
448 and evenness using the Shannon diversity index derived from MODIS data. Nagendra (2002)
449 described landscape diversity as evaluating richness and evenness in the context of measuring
450 diversity. Richness refers to the number of different species (land cover types) in the landscape,
451 and evenness refers to the relative percentage of land distributed amongst these different cover
452 types. The Shannon diversity index of these three case studies shows some change over the
453 period (Appendix J). However, the most prominent change was observed in the farming system
454 of WL1a. The richness and evenness have decreased in WL1a from 2000 to 2019. The evenness
455 values have changed on WM1a in this period. The reasons for these changes would be land
456 fragmentation, land degradation, land-use change, and landslides during this period.

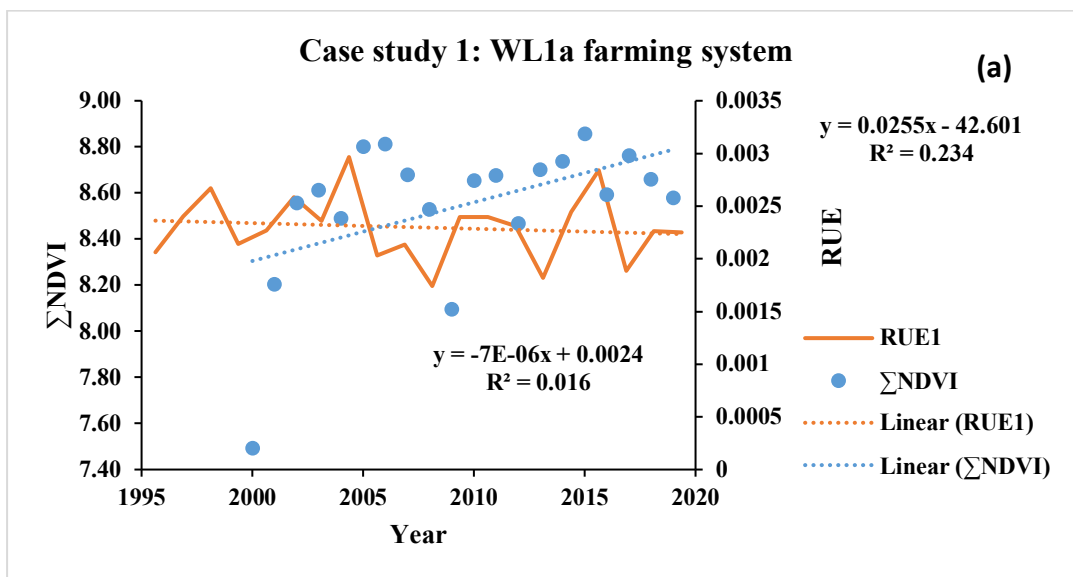
457 NDVI and EVI relationships between rainfalls were also observed. It is somewhat surprising
458 to note a weak correlation between NDVI and rainfall ($r = 0.22$). However, there is a moderate
459 positive correlation between EVI and rainfall ($r = 0.45$) (Appendix I, Table I1). The correlation
460 between NDVI and EVI was observed as $r = 0.36$. Pau et al. (2012) indicated that precipitation

461 and structural complexity strongly affected the correlation between the NDVI and plant
 462 species. Precipitation has a consistent direct effect on the NDVI and species richness. However,
 463 structural complexity has strong direct and indirect effects on the NDVI. The increase in
 464 rainfall would enhance the growth of weeds and crop growth in farming systems. These may
 465 be reasons for the increase in NDVI value in the study. The effect of rainfall can be normalized
 466 by employing rain use efficiency (RUE). Researchers previously highlighted that the RUE
 467 index identifies land degradation that is independent from rainfall (Wessels et al., 2008; Prince
 468 et al., 1998).

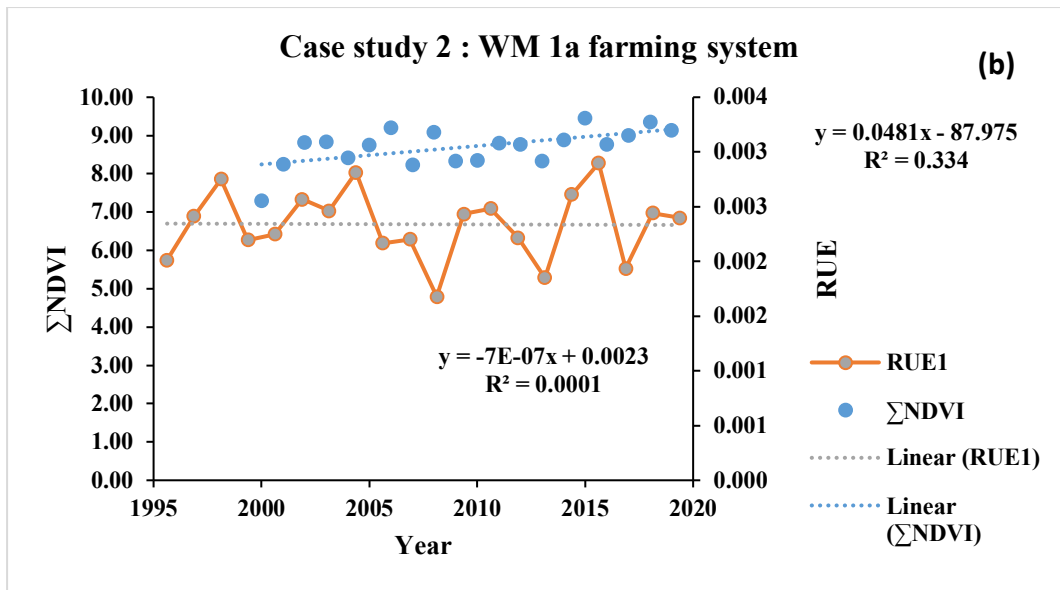
469 4.4.1 Soil erosion hazards and crop diversity change

470 This study estimated the ratio between vegetation indices (VI) and rainfall in the farming
 471 systems of the three case studies. The time series analysis was executed from 2000 to 2019 to
 472 normalize the VI for the influence of rainfall. This is known as rain-use efficiency (RUE). The
 473 ratio between RUE and rainfall can be found in Appendix K (Table K1). Figure 9 shows the
 474 VI and RUE variations for the three case studies.

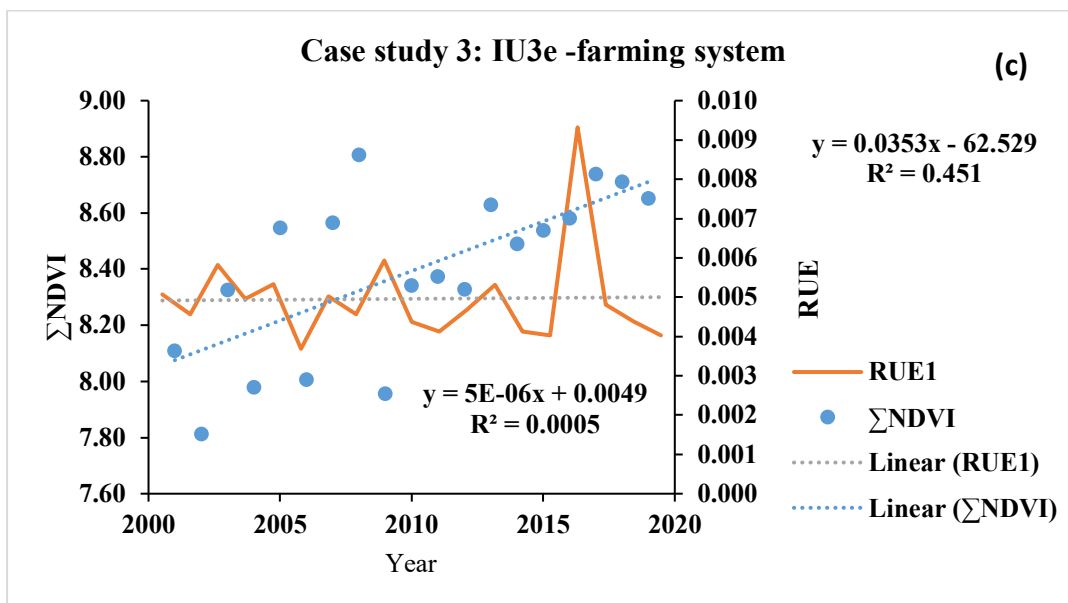
475



476



477



478

479 **Figure 9.** The trend of RUE in three farming systems: (a) WL1a, (b) WM1a, and (c) IU3e
 480 farming systems.

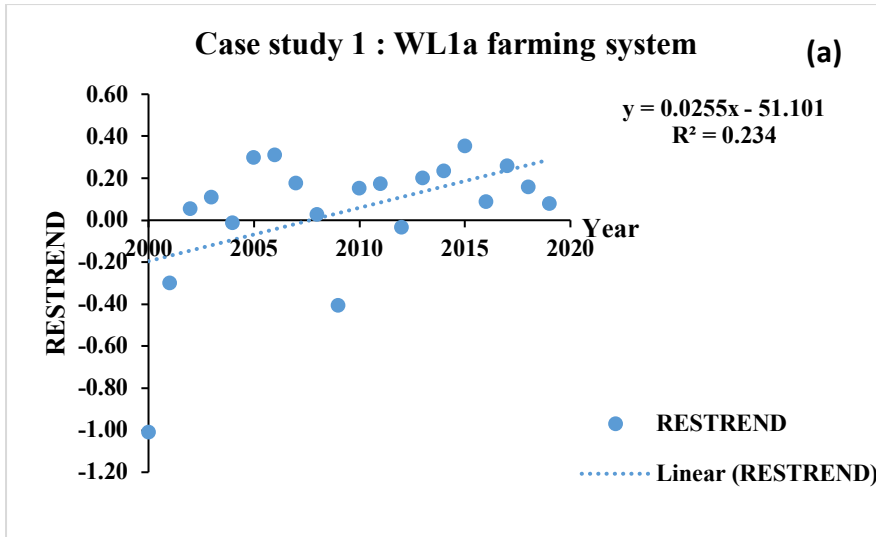
481

482 The farming systems WL1a and WM1a showed a negative trend of the RUE index, while IU3e
 483 showed a positive trend over the years. A similar trend of EVI based RUE ($\Sigma\text{EVI}/\text{rainfall}$) was
 484 also observed in farming systems WL1a and WM1a (see Appendix K, Table K2). The areas
 485 with a negative trend indicated land degradation. It is also noteworthy that these farming
 486 systems receive the highest rainfall compared to the IU3e. The positive trend of RUE in the
 487 IU3e farming system indicates the changes in increasing land cover or land conditions during
 488 the study period. The negative trend may occur due to land-use changes, which reduces NDVI
 489 values. Landmann and Dubovyk (2014) have observed a negative NDVI trend that indicates a
 490 gradual decline of vegetation cover or sudden land transformations such as deforestation.

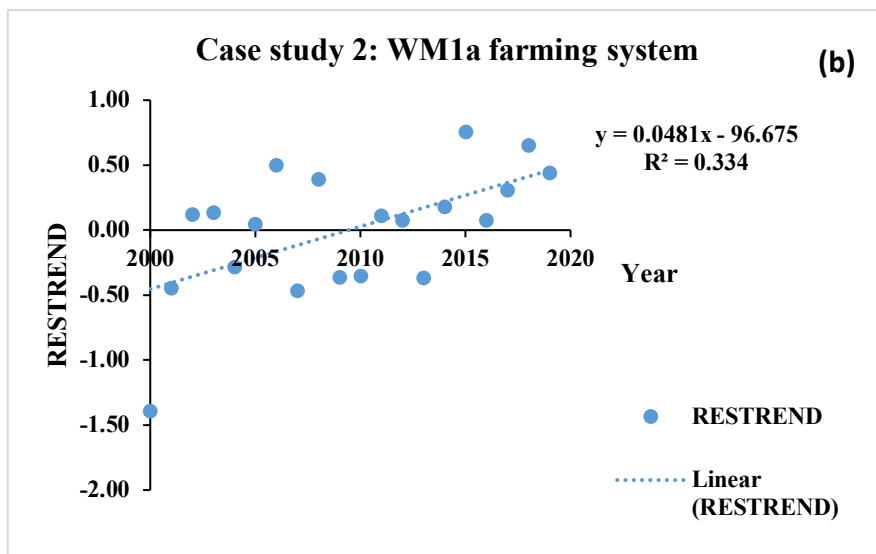
491 This study examined the correlation between RUE and rainfall. There is a strong negative
492 correlation between RUE and rainfall ($r = -0.94$, standard deviation = 0.001). Further to this,
493 the coefficient of determination (R^2) was estimated to find the relationship between RUE, and
494 rainfall. The results show there is a strong negative relationship between RUE and rainfall in
495 three case studies: WL1a ($R^2 = 0.88$), WM1a ($R^2 = 0.78$), and IU3e ($R^2 = 0.86$) (Appendix L,
496 Figure L1).

497 The time-series analysis of MODIS VI was employed to obtain the RESTREND. The
498 RESTREND of the three farming systems has shown a positive slope over the years. The
499 farming system WL1a showed a slightly positive trend of RESTREND ($R^2 = 0.23$). However,
500 the farming systems WM1a and IU3e reported a stronger positive trend of RESTREND
501 $R^2 = 0.33$ and $R^2 = 0.45$, respectively. A similar trend of the EVI based RESTREND was also
502 found in the same farming systems (Appendix K, Table K2). According to Kundu et al. (2017),
503 the positive trend of RESTREND, indicates human interference on the landscape, such as
504 plantation, cropping and agricultural development that supports increasing NDVI values. The
505 findings of this study are also showing a positive trend of RESTREND. Hence, these findings
506 provide evidence to prove the effect of human interference on the improvement of the
507 vegetation cover in the three case studies. Farming system IU3e indicates the highest effect of
508 human interference on the improvement of vegetation cover. Figure 10 shows the trends of
509 RESTREND in the three case studies.

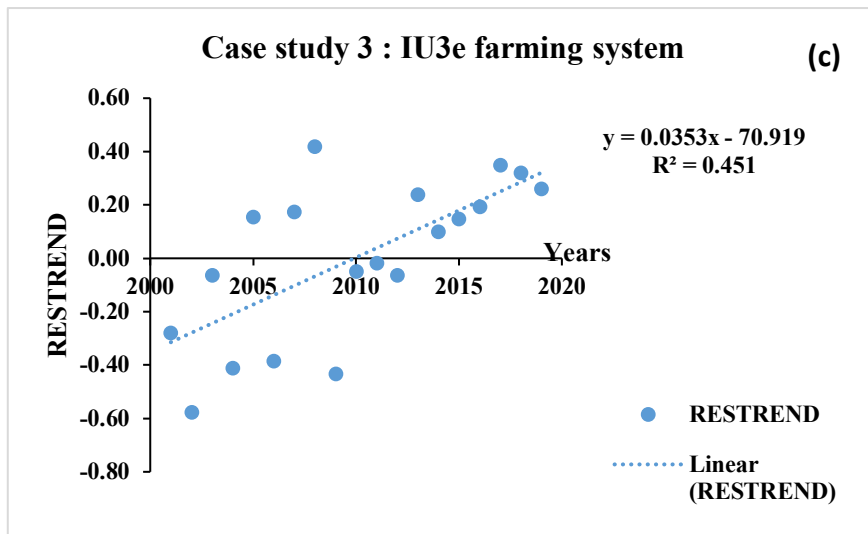
510



511



527



537

538 **Figure 10.** RESTREAND over the years: a) WM1a, b) WL1a, and c) IU3e farming systems.

539 4. Discussion

540 Spatial modeling with four assessments: LULC change, soil erosion hazards, rainfall variation,
541 and crop diversity change assessments were conducted to address the research questions of the
542 study. The LULC evaluation indicates forest and open forest areas have decreased while
543 agricultural and built-up areas have increased during the study period. Other studies also
544 indicated similar findings in their researches (Jayawardena et al., 2018). This study highlighted
545 the large-scale deforestation, which has taken place due to agricultural activities, expansion of
546 home gardens and construction of household settlements. According to a recent study, forest
547 area is decreasing in Sri Lanka (Mondal et al., 2020). Ranasinghe et al. (2019) also confirmed
548 some of these findings, such as decreasing the forest cover and increasing home gardens and
549 agricultural areas in Bandula district of the Central Highlands during the period of 1990 to
550 2018. These findings clearly show the anthropogenic impact on natural ecosystems during the
551 past few decades.

552 According to the RUSLE analysis, the majority of the land area of the Central Highlands, in an
553 ecological and economic sense, has been subjected to soil erosion over the past two decades.
554 The analysis revealed high and very-high soil erosion classes, representing 18.04% of the total
555 land area. The global investigation of modeling and mapping studies (GIMMS) in 1981–2003
556 has indicated 32.09% of the land area was under degradation in Sri Lanka (Bai et al., 2012).
557 The higher rate of soil erosion was evident from the amount of silt piling up behind the dams
558 across the Mahaweli River, which drains through the greater part of the Central Highlands
559 (Khaniya et al., 2019).

560 In addition, the rainfall variation in terms of the increase of rainfall intensity and average
561 rainfall was observed during this study period. A significant increase in rainfall intensity could
562 be observed in Nuwara Eliya. This study found a positive correlation between average annual
563 rainfall and soil erosion. Ratnayake and Herath (2005) claimed spatial locations of recent
564 landslides in the Central Highlands correlate highly with an increase in rainfall intensity. A
565 recent study further revealed a recent incidence of a landslide in the Aranayake area in the
566 Central Highlands, which was triggered by heavy, intense rainfall. This soil mass movement
567 caused great damage in the Aranayake area by killing 127 people and demolishing 75 houses
568 (Dang et al., 2019). However, the impact of climatic variation, particularly rainfall variation in
569 the Central Highlands, is not uniform everywhere.

570 The drastic land-use changes may cause changes in heat and moisture fluxes that would lead
571 to local rainfall variation. In addition, the relationship between rainfall and temperature may
572 be a result of factors such as global warming and land-use change. The increase in sea surface
573 temperature may also be responsible for the increase in rainfall in the western part of the Central
574 Highlands (Wickramagamage, 1998). Scholars indicated the moisture retention capacity of the
575 atmosphere might increase by 7% by increasing global mean temperature from one degree
576 Celsius (Mullan et al., 2012; Almagro et al., 2017). The increasing atmospheric water vapor
577 may change the hydrological cycle and induce more intensive precipitation events (Nearing et
578 al., 2005; Mullan et al., 2012).

579 Studies show that the onset of the two-monsoon pattern (southwest and northeast) in Sri
580 Lanka has also been altered, and the increase of rainfall intensity could be observed in the
581 recent past (Jayawardena et al., 2018; Burt and Weerasinghe, 2014). The changes of onset of
582 monsoons have been affected farming activities in the Central Highlands. The smallholdings
583 and rain-fed agriculture dominate the Central Highlands. Borrelli et al. (2017) also highlighted
584 that the most severe impacts of global climate change would be felt mostly on smallholder
585 farmers in developing countries.

586 The NDVI, EVI and standard deviations of GPP across the highlands were used as measures
587 of vegetation heterogeneity. Ecosystem productivity has shown a good correlation with species
588 diversity, as it is the integrative expression of factors such as topography, land use, disturbance,
589 and soil nutrients (Evans and Geerken, 2004; John et al., 2008). As a measure of plant diversity,
590 plant species richness is often considered a measure of ecosystem health and resilience
591 (Symstad and Jonas, 2011). Pohl et al. (2009) indicated that plant species richness significantly
592 increased the topsoil aggregate stability on slopes.

593 In the crop diversity assessment of this study, NDVI was normalized by rainfall (RUE index).
594 Findings show a decreasing trend of RUE in WL1a and WM1a farming systems. Further to
595 this, soil erosion of these two farming systems is also high. Previous research emphasizes that
596 a decreasing trend of RUE indicates land degradation that is independent from rainfall (Wessels
597 et al., 2008; Prince et al., 1998). Thus, the findings of this study confirmed the land degradation
598 in WL1a and WM1a farming systems. Levin et al. (2007) found that a decreasing trend of
599 vegetation indices would be an indication of the decreasing heterogeneity or species diversity.
600 The Shannon index (plant richness and evenness) in the WL1a and WM1a farming systems
601 (western part of the Central Highlands) also decreases. Hence, the present study provides

602 evidence for the decreasing of crop diversity. Besides, crop diversity in farmland can vary due
603 to various reasons, such as socio-economic factors. Farmers would shift from one crop to
604 another crop due to changes in market prices (Maitima et al., 2009), environmental influences
605 or socio-economic factors in farming systems (Shrestha et al., 2010). Therefore, further
606 assessment and ground-based validation are needed to generalize the correlation between soil
607 erosion and plant diversity change.

608 The study further investigated land degradation using RESTREND analysis to distinguish
609 human-induced land degradation. To interpret the NDVI trends in terms of land degradation or
610 improvement, researchers have to eliminate the impact of climatic variability from the residual
611 sum of NDVI to detect human influence (Wessels et al., 2007; Kundu et al., 2017). A negative
612 trend of RESTREND indicates human-induced land degradation, while a positive trend of
613 RESTREND indicates human influences on the improvement of vegetation (Kundu et al., 2017;
614 Evans, 2004). The present study demonstrates an increasing trend of RESTREND, which
615 means an improvement of vegetation cover in the farming systems. Findings provide evidence
616 to prove the effect of human interference on the improvement of vegetation in three case
617 studies.

618 The increasing farming areas, improved farming techniques, and land reclamation may be the
619 reasons for improving vegetation cover. Similarly, Burrell et al. (2017) found that certain
620 farming practices such as fertilizer applications, irrigation, high breed varieties of seasonal
621 crops, etc. significantly increase the NDVI values. Fensholt et al. (2013) described trends of
622 vegetation productivity as dependent on climatic factors and non-climatic factors such as land
623 management, cropping practices, and nutrient status. Climatic factors are precipitation,
624 atmospheric temperature, global sea surface temperature, and soil moisture (Fensholt et al.,
625 2013; Ibrahim et al., 2015). Burrell et al. (2017) and other researchers argued that increasing
626 trends of vegetation cover due to the long-term increasing trend of rainfall or CO₂ fertilization
627 due to anthropogenic greenhouse gas emissions (Sarmah et al., 2018; Anyamba and Tucker,
628 2005).

629 There are several important areas in this study that make an original contribution to the body
630 of knowledge; extraction of farming systems based on the agro-ecological regions, application
631 of rain use efficiency and trend analysis for land degradation in farming systems, and residual
632 trend analysis to distinguish the human-induced land degradation at a farming system level. To
633 the best of the knowledge of the authors of this paper, no studies have previously been

634 conducted to integrate these aspects at a farming system level in Sri Lanka. The present study
635 gives a novel spatial modeling approach by combining LULC, soil erosion hazards, crop
636 diversity change, and rainfall variation. Moreover, this study provides comprehensive scientific
637 insights into sustainable land and farming system management. These insights are very critical
638 in developing strategies to ensure food security and sustainable land management (Visser et
639 al., 2019; Djekic et al., 2021). In other words, food security and sustainable land management
640 are paramount two aspects in achieving sustainable development goals (SGDs) and 2030
641 agenda: particularly in achieving goals 2 and 15 (Zero hunger and Life on land). Hence, this
642 research contributes to developing strategies in achieving SGDs of the United Nations.
643 However, there are some limitations to this study. The relationship between rainfall and plant
644 water availability is not a simple process, and only a fraction of the rainfall, becomes available
645 for transpiration and evaporation. These parameters did not consider in this study. In addition,
646 an increase in temperature and CO₂ changes were also not considered.

647 The model developed by this study can be used for early detection and to reduce the potential
648 adverse impact of climate change and future damages to farming systems. Hence, this approach
649 provides a basis for a new direction for future research. The policy implication of this study
650 provides a direction towards developing strategies for land management and resilience
651 building, guiding future land-use planning for the soil and ecological conservation in areas
652 under high and very high soil erosion categories to protect the farming systems sustainably.
653 The significance of this study implies an improved understanding of soil erosion hazards
654 caused by rainfall variation and crop diversity changes through remote sensing applications,
655 accompanied to formulate climate risk management strategies and mitigation measures for
656 better management of farming systems and risk reduction.

657 **5. Conclusion**

658 This paper presents time-series segmentation of LULC change, soil erosion hazards, crop
659 diversity change, and rainfall variation in the Central Highlands of Sri Lanka from 2000 to
660 2019. The LULC indicates agricultural lands (15.4%) and built-up areas (2.35%) have been
661 increasing while reducing the dense forest(14.5%) and open forest cover(5.8%). The soil
662 erosion has increased from 9.08 Mg/ha/yr to 11.08 Mg/ha/yr. The rainfall variation revealed a
663 significantly increasing trend. Crop diversity has also been decreased in the WL1a (SHDI from
664 0.45 to 0.41) and WM1a (SHDI from 0.69 to 0.65) farming systems. Furthermore, a positive
665 trend of RESTREND is reported in WL1a ,WM1a and IU3e farming systems. This is evidence

666 to prove the effect of human interference on the improvement of vegetation in the WL1a,
667 WM1a and IU3e farming systems. It suggests climate-induced soil erosion may be responsible
668 for land degradation in these farming systems. These findings imply the complex relationships
669 among soil erosion, plant diversity change and rainfall variation. The combined spatial
670 modeling approach provides a better understanding of the ground situation and can predict the
671 situation with a meaningful outcome. Remote sensing derived NDVI and EVI indices provide
672 the best solution for monitoring vegetation cover and plant diversity change. Overall, these
673 findings are evidence that human-induced LULC change and climate-induced land degradation
674 create significant damage to farming systems that greatly threaten the food production of the
675 Central Highlands of Sri Lanka.

676 **Funding:** The research is supported by the Centre for Advanced Modeling and Geospatial
677 Information Systems (CAMGIS), Faculty of Engineering & IT, University of Technology
678 Sydney.

679 **Author Contributions:** Conceptualization, S.S. and B.P.; methodology, S.S., B.P.; software,
680 S.S., B.P., A.H.; validation, S.S.; formal analysis, S.S.; writing—original draft preparation,
681 S.S.; writing—review and editing, S.S., B.P., A.H. and J.B.; supervision, B.P., A.H. and J.B.;
682 funding acquisition, B.P.

683 **Declaration of Competing Interest:** The authors declare that they have no known competing
684 financial interests or personal relationships that could have appeared to influence the work
685 reported in this paper.

686 Reference

- 687 Alewell, C., Borrelli, P., Meusburger, K., Panagos, P., 2019. Using the USLE: Chances,
688 challenges and limitations of soil erosion modelling. *Int. Soil Water Conserv. Res.*
689 <https://doi.org/10.1016/j.iswcr.2019.05.004>
- 690 Almagro, A., Oliveira, P.T.S., Nearing, M.A., Hagemann, S., 2017. Projected climate change
691 impacts in rainfall erosivity over Brazil. *Sci. Rep.* 7, 1–12.
692 <https://doi.org/10.1038/s41598-017-08298-y>
- 693 Angima, S.D., Stott, D.E., O'Neill, M.K., Ong, C.K., Weesies, G.A., 2003. Soil erosion
694 prediction using RUSLE for central Kenyan highland conditions. *Agric. Ecosyst. Environ.*
695 97, 295–308. [https://doi.org/10.1016/S0167-8809\(03\)00011-2](https://doi.org/10.1016/S0167-8809(03)00011-2)
- 696 Anyamba, A., Tucker, C.J., 2005. Analysis of Sahelian vegetation dynamics using NOAA-
697 AVHRR NDVI data from 1981-2003, in: *Journal of Arid Environments*. Academic Press,

698 pp. 596–614. <https://doi.org/10.1016/j.jaridenv.2005.03.007>

699 Auerswald, K., Menzel, A., 2021. Change in erosion potential of crops due to climate change.
700 *Agric. For. Meteorol.* 300, 108338. <https://doi.org/10.1016/j.agrformet.2021.108338>

701 Baez-Villanueva, O.M., Zambrano-Bigiarini, M., Ribbe, L., Nauditt, A., Giraldo-Osorio, J.D.,
702 Thinh, N.X., 2018. Temporal and spatial evaluation of satellite rainfall estimates over
703 different regions in Latin-America. *Atmos. Res.* 213, 34–50.
704 <https://doi.org/10.1016/j.atmosres.2018.05.011>

705 Bai, Z.G., Conijn, J.G., Bindraban, P.S., Rutgers, B., 2012. Global changes of remotely sensed
706 greenness and simulated biomass production since 1981: towards mapping global soil
707 degradation. Rep. - ISRIC World Soil Inf. 33 pp.

708 Berendse, F., van Ruijven, J., Jongejans, E., Keesstra, S., 2015. Loss of plant species diversity
709 reduces soil erosion resistance. *Ecosystems* 18, 881–888. [https://doi.org/10.1007/s10021-](https://doi.org/10.1007/s10021-015-9869-6)
710 [015-9869-6](https://doi.org/10.1007/s10021-015-9869-6)

711 Bishop, Y.M., Holland, P.W., Fienberg, S.E., 2007. Discrete multivariate analysis theory and
712 practice, *Discrete Multivariate Analysis Theory and Practice*. Springer New York.
713 <https://doi.org/10.1007/978-0-387-72806-3>

714 Borrelli, P., Panagos, P., 2020. An indicator to reflect the mitigating effect of Common
715 Agricultural Policy on soil erosion. *Land use policy* 92, 104467.
716 <https://doi.org/10.1016/j.landusepol.2020.104467>

717 Borrelli, P., Robinson, D.A., Fleischer, L.R., Lugato, E., Ballabio, C., Alewell, C., Meusburger,
718 K., Modugno, S., Schütt, B., Ferro, V., Bagarello, V., Oost, K. Van, Montanarella, L.,
719 Panagos, P., 2017. An assessment of the global impact of 21st century land use change on
720 soil erosion. *Nat. Commun.* 8, 2017. <https://doi.org/10.1038/s41467-017-02142-7>

721 Burrell, A.L., Evans, J.P., Liu, Y., 2017. Detecting dryland degradation using Time Series
722 Segmentation and Residual Trend analysis (TSS-RESTREND). *Remote Sens. Environ.*
723 197, 43–57. <https://doi.org/10.1016/j.rse.2017.05.018>

724 Burt, T.P., Weerasinghe, K.D.N., 2014. Rainfall distributions in Sri Lanka in time and space:
725 An analysis based on daily rainfall data. *Climate* 2, 242–263.
726 <https://doi.org/10.3390/cli2040242>

727 Chander, G., Markham, B.L., Helder, D.L., 2009. Summary of current radiometric calibration
728 coefficients for Landsat MSS, TM, ETM+, and EO-1 ALI sensors. *Remote Sens. Environ.*
729 113, 893–903. <https://doi.org/10.1016/j.rse.2009.01.007>

730 Chavez, P.S., 1996. Image-based atmospheric corrections - Revisited and improved.
731 *Photogramm. Eng. Remote Sensing* 62, 1025–1036.

732 Chitale, V.S., Behera, M.D., Roy, P.S., 2019. Deciphering plant richness using satellite remote
733 sensing: a study from three biodiversity hotspots. *Biodivers. Conserv.* 28, 2183–2196.
734 <https://doi.org/10.1007/s10531-019-01761-4>

735 Cortes, C., Vapnik, V., 1995. Support-vector networks. *Mach. Learn.* 20, 273–297.
736 <https://doi.org/10.1007/bf00994018>

737 Cunha, J., Nóbrega, R.L.B., Rufino, I., Erasmi, S., Galvão, C., Valente, F., 2020. Surface
738 albedo as a proxy for land-cover clearing in seasonally dry forests: Evidence from the
739 Brazilian Caatinga. *Remote Sens. Environ.* 238, 111250.
740 <https://doi.org/10.1016/j.rse.2019.111250>

741 Dang, K., Sassa, K., Konagai, K., Karunawardena, A., Bandara, R.M.S., Hirota, K., Tan, Q.,
742 Ha, N.D., 2019. Recent rainfall-induced rapid and long-traveling landslide on 17 May
743 2016 in Aranayaka, Kagelle District, Sri Lanka. *Landslides* 16, 155–164.
744 <https://doi.org/10.1007/s10346-018-1089-7>

745 Djekic, I., Batlle-Bayer, L., Bala, A., Fullana-I-palmer, P., Jambrak, A.R., 2021. Role of the
746 food supply chain stakeholders in achieving un sdgs. *Sustain.* 13.
747 <https://doi.org/10.3390/su13169095>

748 Eckstein, D., Wings, M., Marie-Lena, H., 2019. Global climate risk index 2019 [WWW
749 Document]. URL <https://germanwatch.org/en/16046> (accessed 5.8.21).

750 Esham, M., Garforth, C., 2013. Climate change and agricultural adaptation in Sri Lanka: A
751 review. *Clim. Dev.* <https://doi.org/10.1080/17565529.2012.762333>

752 Evans, J., Geerken, R., 2004. Discrimination between climate and human-induced dryland
753 degradation. *J. Arid Environ.* 57, 535–554. [https://doi.org/10.1016/S0140-](https://doi.org/10.1016/S0140-1963(03)00121-6)
754 [1963\(03\)00121-6](https://doi.org/10.1016/S0140-1963(03)00121-6)

755 Fensholt, R., Rasmussen, K., Kaspersen, P., Huber, S., Horion, S., Swinnen, E., 2013.
756 Assessing land degradation/recovery in the african sahel from long-term earth observation
757 based primary productivity and precipitation relationships. *Remote Sens.* 5, 664–686.
758 <https://doi.org/10.3390/rs5020664>

759 Fenta, A.A., Tsunekawa, A., Haregeweyn, N., Tsubo, M., Yasuda, H., Kawai, T., Ebabu, K.,
760 Berihun, M.L., Belay, A.S., Sultan, D., 2021. Agroecology-based soil erosion assessment
761 for better conservation planning in Ethiopian river basins. *Environ. Res.* 195, 110786.
762 <https://doi.org/10.1016/j.envres.2021.110786>

763 Fernández, C., Vega, J.A., 2018. Evaluation of the rusle and disturbed wepp erosion models
764 for predicting soil loss in the first year after wildfire in NW Spain. *Environ. Res.* 165,
765 279–285. <https://doi.org/10.1016/j.envres.2018.04.008>

766 Ganasri, B.P., Ramesh, H., 2016. Assessment of soil erosion by RUSLE model using remote
767 sensing and GIS - A case study of Nethravathi Basin. *Geosci. Front.* 7, 953–961.
768 <https://doi.org/10.1016/j.gsf.2015.10.007>

769 Gupta, H. V., Kling, H., Yilmaz, K.K., Martinez, G.F., 2009. Decomposition of the mean
770 squared error and NSE performance criteria: Implications for improving hydrological
771 modelling. *J. Hydrol.* 377, 80–91. <https://doi.org/10.1016/j.jhydrol.2009.08.003>

772 Han, J., Ge, W., Hei, Z., Cong, C., Ma, C., Xie, M., Liu, B., Feng, W., Wang, F., Jiao, J., 2020.
773 Agricultural land use and management weaken the soil erosion induced by extreme
774 rainstorms. *Agric. Ecosyst. Environ.* 301, 107047.
775 <https://doi.org/10.1016/j.agee.2020.107047>

776 Hewawasam, T., 2010. Effect of land use in the upper Mahaweli catchment area on erosion
777 landslides and siltation in hydropower reservoirs of Sri Lanka. *J. Natl. Sci. Found. Sri
778 Lanka* 38, 3–14. <https://doi.org/10.4038/jnsfsr.v38i1.1721>

779 Hewawasam, T., Illangasinghe, S., 2015. Quantifying sheet erosion in agricultural highlands
780 of Sri Lanka by tracking grain-size distributions. *Anthropocene* 11, 25–34.
781 <https://doi.org/10.1016/j.ancene.2015.11.004>

782 Hewawasam, T., von Blanckenburg, F., Bouchez, J., Dixon, J.L., Schuessler, J.A., Maekeler,
783 R., 2013. Slow advance of the weathering front during deep, supply-limited saprolite
784 formation in the tropical Highlands of Sri Lanka. *Geochim. Cosmochim. Acta* 118, 202–
785 230. <https://doi.org/10.1016/j.gca.2013.05.006>

786 Hou, J., Wang, H., Fu, B., Zhu, L., Wang, Y., Li, Z., 2016. Effects of plant diversity on soil
787 erosion for different vegetation patterns. *Catena* 147, 632–637.
788 <https://doi.org/10.1016/j.catena.2016.08.019>

789 Huete, A., Didan, K., Miura, T., Rodriguez, E.P., Gao, X., Ferreira, L.G., 2002. Overview of
790 the radiometric and biophysical performance of the MODIS vegetation indices. *Remote
791 Sens. Environ.* 83, 195–213. [https://doi.org/10.1016/S0034-4257\(02\)00096-2](https://doi.org/10.1016/S0034-4257(02)00096-2)

792 Huete, A.R., 1988. A soil-adjusted vegetation index (SAVI). *Remote Sens. Environ.* 25, 295–
793 309. [https://doi.org/10.1016/0034-4257\(88\)90106-X](https://doi.org/10.1016/0034-4257(88)90106-X)

794 Hunt, N.D., Hill, J.D., Liebman, M., 2019. Cropping System Diversity Effects on Nutrient
795 Discharge, Soil Erosion, and Agronomic Performance. *Environ. Sci. Technol.* 53, 1344–
796 1352. <https://doi.org/10.1021/acs.est.8b02193>

797 Ibrahim, Y.Z., Balzter, H., Kaduk, J., Tucker, C.J., 2015. Land degradation assessment using
798 residual trend analysis of GIMMS NDVI3g, soil moisture and rainfall in Sub-Saharan
799 West Africa from 1982 to 2012. *Remote Sens.* 7, 5471–5494.

800 <https://doi.org/10.3390/rs70505471>

801 Jayawardena, I.M.S.P., Darshika, D.W.T.T., C. Herath, H.M.R., 2018. Recent Trends in
802 Climate Extreme Indices over Sri Lanka. *Am. J. Clim. Chang.* 07, 586–599.
803 <https://doi.org/10.4236/ajcc.2018.74036>

804 John, R., Chen, J., Lu, N., Guo, K., Liang, C., Wei, Y., Noormets, A., Ma, K., Han, X., 2008.
805 Predicting plant diversity based on remote sensing products in the semi-arid region of
806 Inner Mongolia. *Remote Sens. Environ.* 112, 2018–2032.
807 <https://doi.org/10.1016/j.rse.2007.09.013>

808 Khaniya, B., Jayanayaka, I., Jayasanka, P., Rathnayake, U., 2019. Rainfall Trend Analysis in
809 Uma Oya Basin, Sri Lanka, and Future Water Scarcity Problems in Perspective of Climate
810 Variability. *Adv. Meteorol.* 2019. <https://doi.org/10.1155/2019/3636158>

811 Kling, J.R., Mullainathan, S., Shafir, E., Vermeulen, L.C., Wrobel, M. V., 2012. Comparison
812 friction: Experimental evidence from medicare drug plans. *Q. J. Econ.* 127, 199–235.
813 <https://doi.org/10.1093/qje/qjr055>

814 Kundu, A., Patel, N.R., Saha, S.K., Dutta, D., 2017. Desertification in western Rajasthan
815 (India): an assessment using remote sensing derived rain-use efficiency and residual trend
816 methods. *Nat. Hazards* 86, 297–313. <https://doi.org/10.1007/s11069-016-2689-y>

817 Lal, R., 2011. Climate of South Asia and the Human Wellbeing, in: *Climate Change and Food*
818 *Security in South Asia*. Springer Netherlands, pp. 3–12. [https://doi.org/10.1007/978-90-](https://doi.org/10.1007/978-90-481-9516-9_1)
819 [481-9516-9_1](https://doi.org/10.1007/978-90-481-9516-9_1)

820 Landmann, T., Dubovyk, O., 2014. Spatial analysis of human-induced vegetation productivity
821 decline over eastern Africa using a decade (2001-2011) of medium resolution MODIS
822 time-series data. *Int. J. Appl. Earth Obs. Geoinf.* 33, 76–82.
823 <https://doi.org/10.1016/j.jag.2014.04.020>

824 Lee, S., Talib, J.A., 2005. Probabilistic landslide susceptibility and factor effect analysis.
825 *Environ. Geol.* 47, 982–990. <https://doi.org/10.1007/s00254-005-1228-z>

826 Levin, N., Shmida, A., Levanoni, O., Tamari, H., Kark, S., 2007. Predicting mountain plant
827 richness and rarity from space using satellite-derived vegetation indices. *Divers. Distrib.*
828 13, 692–703. <https://doi.org/10.1111/j.1472-4642.2007.00372.x>

829 Liu, H.Q., Huete, A., 1996. A feedback based modification of the NDVI to minimize canopy
830 background and atmospheric noise. *IEEE Trans. Geosci. Remote Sens.* 33, 457–465.
831 <https://doi.org/10.1109/tgrs.1995.8746027>

832 Liu, J., Gao, G., Wang, S., Jiao, L., Wu, X., Fu, B., 2018. The effects of vegetation on runoff
833 and soil loss: Multidimensional structure analysis and scale characteristics. *J. Geogr. Sci.*

834 28, 59–78. <https://doi.org/10.1007/s11442-018-1459-z>

835 Liu, Y., Li, Y., Li, S., Motesharrei, S., 2015. Spatial and temporal patterns of global NDVI
836 trends: Correlations with climate and human factors. *Remote Sens.* 7, 13233–13250.
837 <https://doi.org/10.3390/rs71013233>

838 LPDAAC, 2021. Land Processes Distributed Active Archive Center [WWW Document].
839 NASA EOSDIS L. Process. DAAC, USGS Earth Resour. Obs. Sci. Center, Sioux Falls,
840 South Dakota. URL <https://lpdaac.usgs.gov/> (accessed 6.20.21).

841 Maitima, J.M., Mugatha, S.M., Reid, R.S., Gachimbi, L.N., Majule, A., Lyaruu, H., Pomery,
842 D., Mathai, S., Mugisha, S., 2009. The linkages between land use change, land
843 degradation and biodiversity across East Africa. *African J. Environ. Sci. Technol.* 3, 310–
844 325. <https://doi.org/10.5897/AJEST08.173>

845 McLeod, A., McLeod, M., 2014. Package “Kendall,” cran.microsoft.com.

846 Meena, S.R., Ghorbanzadeh, O., Blaschke, T., 2019. A comparative study of statistics-based
847 landslide susceptibility models: A case study of the region affected by the Gorkha
848 earthquake in Nepal. *ISPRS Int. J. Geo-Information* 8.
849 <https://doi.org/10.3390/ijgi8020094>

850 Mondal, P., McDermid, S.S., Qadir, A., 2020. A reporting framework for Sustainable
851 Development Goal 15: Multi-scale monitoring of forest degradation using MODIS,
852 Landsat and Sentinel data. *Remote Sens. Environ.* 237.
853 <https://doi.org/10.1016/j.rse.2019.111592>

854 Morisette, J.T., Jarnevich, C.S., Ullah, A., Cai, W., Pedelty, J.A., Gentle, J.E., Stohlgren, T.J.,
855 Schnase, J.L., 2006. A tamarisk habitat suitability map for the continental United States.
856 *Front. Ecol. Environ.* 4, 11–17. [https://doi.org/10.1890/1540-9295\(2006\)004\[0012:ATHSMF\]2.0.CO;2](https://doi.org/10.1890/1540-9295(2006)004[0012:ATHSMF]2.0.CO;2)

857

858 Mullan, D., Favis-Mortlock, D., Fealy, R., 2012. Addressing key limitations associated with
859 modelling soil erosion under the impacts of future climate change. *Agric. For. Meteorol.*
860 156, 18–30. <https://doi.org/10.1016/j.agrformet.2011.12.004>

861 Nagendra, H., 2002. Opposite trends in response for the Shannon and Simpson indices of
862 landscape diversity. *Appl. Geogr.* 22, 175–186. [https://doi.org/10.1016/S0143-6228\(02\)00002-4](https://doi.org/10.1016/S0143-6228(02)00002-4)

863

864 Nagendra, H., Rocchini, D., Ghate, R., Sharma, B., Pareeth, S., 2010. Assessing plant diversity
865 in a dry tropical forest: Comparing the utility of landsat and ikonos satellite images.
866 *Remote Sens.* 2, 478–496. <https://doi.org/10.3390/rs2020478>

867 Nampak, H., Pradhan, B., Mojaddadi Rizeei, H., Park, H.J., 2018. Assessment of land cover

868 and land use change impact on soil loss in a tropical catchment by using multitemporal
869 SPOT-5 satellite images and Revised Universal Soil Loss Equation model. *L. Degrad.*
870 *Dev.* 29, 3440–3455. <https://doi.org/10.1002/ldr.3112>

871 Nay, J., Burchfield, E., Gilligan, J., 2018. A machine-learning approach to forecasting remotely
872 sensed vegetation health. *Int. J. Remote Sens.* 39, 1800–1816.
873 <https://doi.org/10.1080/01431161.2017.1410296>

874 Nearing, M.A., Jetten, V., Baffaut, C., Cerdan, O., Couturier, A., Hernandez, M., Le
875 Bissonnais, Y., Nichols, M.H., Nunes, J.P., Renschler, C.S., Souchère, V., Van Oost, K.,
876 2005. Modeling response of soil erosion and runoff to changes in precipitation and cover,
877 in: *Catena*. Elsevier, pp. 131–154. <https://doi.org/10.1016/j.catena.2005.03.007>

878 Olofsson, P., Foody, G.M., Stehman, S. V., Woodcock, C.E., 2013. Making better use of
879 accuracy data in land change studies: Estimating accuracy and area and quantifying
880 uncertainty using stratified estimation. *Remote Sens. Environ.* 129, 122–131.
881 <https://doi.org/10.1016/j.rse.2012.10.031>

882 ORNL DAAC, 2018. MODIS and VIIRS Land Products Global Subsetting and Visualization
883 Tool [WWW Document]. ORNL DAAC, Oak Ridge, Tennessee, USA. URL
884 https://daac.ornl.gov/cgi-bin/dsviewer.pl?ds_id=1379 (accessed 6.25.21).

885 Panagos, P., Katsoyiannis, A., 2019. Soil erosion modelling: The new challenges as the result
886 of policy developments in Europe. *Environ. Res.*
887 <https://doi.org/10.1016/j.envres.2019.02.043>

888 Pau, S., Gillespie, T.W., Wolkovich, E.M., 2012. Dissecting NDVI-species richness
889 relationships in Hawaiian dry forests. *J. Biogeogr.* 39, 1678–1686.
890 <https://doi.org/10.1111/j.1365-2699.2012.02731.x>

891 Pohl, M., Alig, D., Körner, C., Rixen, C., 2009. Higher plant diversity enhances soil stability
892 in disturbed alpine ecosystems. *Plant Soil* 324, 91–102. [https://doi.org/10.1007/s11104-](https://doi.org/10.1007/s11104-009-9906-3)
893 [009-9906-3](https://doi.org/10.1007/s11104-009-9906-3)

894 Pouteau, R., Gillespie, T.W., Birnbaum, P., 2018. Predicting tropical tree species richness from
895 normalized difference vegetation index time series: The devil is perhaps not in the detail.
896 *Remote Sens.* 10, 698. <https://doi.org/10.3390/rs10050698>

897 Pradhan, B., Chaudhari, A., Adinarayana, J., Buchroithner, M.F., 2012. Soil erosion
898 assessment and its correlation with landslide events using remote sensing data and GIS:
899 A case study at Penang Island, Malaysia. *Environ. Monit. Assess.* 184, 715–727.
900 <https://doi.org/10.1007/s10661-011-1996-8>

901 Prince, S.D., Colstoun, E.B.D., Kravitz, L.L., 1998. Evidence from rain-use efficiencies does

902 not indicate extensive Sahelian desertification. *Glob. Chang. Biol.* 4, 359–374.
903 <https://doi.org/10.1046/j.1365-2486.1998.00158.x>

904 Qi, Z., Yeh, A.G.O., Li, X., Lin, Z., 2012. A novel algorithm for land use and land cover
905 classification using RADARSAT-2 polarimetric SAR data. *Remote Sens. Environ.* 118,
906 21–39. <https://doi.org/10.1016/j.rse.2011.11.001>

907 Ranasinghe, A.K.R.N., Bandara, R., Puswewala, U.G.A., Dammalage, T.L., 2019. Efficacy of
908 using Radar Induced Factors in Landslide Susceptibility Analysis: case study of Koslanda,
909 Sri Lanka. *Nat. Hazards Earth Syst. Sci. Discuss.* 1–22. [https://doi.org/10.5194/nhess-](https://doi.org/10.5194/nhess-2018-335)
910 [2018-335](https://doi.org/10.5194/nhess-2018-335)

911 Rathnayake, C.W., Jones, S., Soto-Berelev, M., 2020. Mapping land cover change over a 25-
912 year period (1993-2018) in Sri Lanka using landsat time-series. *Land* 9, 27.
913 <https://doi.org/10.3390/land9010027>

914 Ratna, S.B., Cherchi, A., Osborn, T.J., Joshi, M., Uppara, U., 2021. The Extreme Positive
915 Indian Ocean Dipole of 2019 and Associated Indian Summer Ratna, Satyaban B., Annalisa
916 Cherchi, Timothy J. Osborn, Manoj Joshi, and Umakanth Uppara. 2021. “The Extreme
917 Positive Indian Ocean Dipole of 2019 and Associated Indian Summer Mo. *Geophys. Res.*
918 *Lett.* <https://doi.org/10.1029/2020GL091497>

919 Ratnayake, U., Herath, S., 2005. Changing rainfall and its impact on landslides in Sri Lanka.
920 *J. Mt. Sci.* 2, 218–224. <https://doi.org/10.1007/bf02973195>

921 Rizeei, H.M., Saharkhiz, M.A., Pradhan, B., Ahmad, N., 2016. Soil erosion prediction based
922 on land cover dynamics at the Semenyih watershed in Malaysia using LTM and USLE
923 models. *Geocarto Int.* 31, 1158–1177. <https://doi.org/10.1080/10106049.2015.1120354>

924 Rouse, J.W., Haas, R.H., Schell, J.A., Deering, D.W., 1974. Monitoring Vegetation Systems
925 in the Great Plains with ERTS, in: Stanley C. Freden, Enrico P. Mercanti, and M.A.B. (Ed.),
926 Third Earth Resources Technology Satellite-1 Symposium- Volume I: Technical
927 Presentations. NASA SP. published by NASA, Washington, D.C., Washington, D.C.,
928 USA, p. 309.

929 Rozos, D., Skilodimou, H.D., Loupasakis, C., Bathrellos, G.D., 2013. Application of the
930 revised universal soil loss equation model on landslide prevention. An example from N.
931 Euboea (Evia) Island, Greece. *Environ. Earth Sci.* 70, 3255–3266.
932 <https://doi.org/10.1007/s12665-013-2390-3>

933 Sadeghi, M., Nguyen, P., Naeini, M.R., Hsu, K., Braithwaite, D., Sorooshian, S., 2021.
934 PERSIANN-CCS-CDR, a 3-hourly 0.04° global precipitation climate data record for
935 heavy precipitation studies. *Sci. Data* 8. <https://doi.org/10.1038/s41597-021-00940-9>

936 Sarmah, S., Jia, G., Zhang, A., 2018. Satellite view of seasonal greenness trends and controls
937 in South Asia. *Environ. Res. Lett.* 13. <https://doi.org/10.1088/1748-9326/aaa866>

938 Şen, Z., 2012. Innovative Trend Analysis Methodology. *J. Hydrol. Eng.* 17, 1042–1046.
939 [https://doi.org/10.1061/\(asce\)he.1943-5584.0000556](https://doi.org/10.1061/(asce)he.1943-5584.0000556)

940 Senanayake, S., Pradhan, B., Huete, A., Brennan, J., 2021. Proposing an ecologically viable
941 and economically sound farming system using a matrix-based geo-informatics approach.
942 *Sci. Total Environ.* 794, 148788. <https://doi.org/10.1016/j.scitotenv.2021.148788>

943 Senanayake, S., Pradhan, B., Huete, A., Brennan, J., 2020a. A Review on Assessing and
944 Mapping Soil Erosion Hazard Using Geo-Informatics Technology for Farming System
945 Management. *Remote Sens.* 12, 4063. <https://doi.org/10.3390/rs12244063>

946 Senanayake, S., Pradhan, B., Huete, A., Brennan, J., 2020b. Assessing Soil Erosion Hazards
947 Using Land-Use Change and Landslide Frequency Ratio Method: A Case Study of
948 Sabaragamuwa Province, Sri Lanka. *Remote Sens.* 12, 1483.
949 <https://doi.org/10.3390/rs12091483>

950 Shannon, C.E., 1948. A Mathematical Theory of Communication. *Bell Syst. Tech. J.* 27, 379–
951 423. <https://doi.org/10.1002/j.1538-7305.1948.tb01338.x>

952 Shrestha, R.P., Schmidt-Vogt, D., Gnanavelrajah, N., 2010. Relating plant diversity to biomass
953 and soil erosion in a cultivated landscape of the eastern seaboard region of Thailand. *Appl.*
954 *Geogr.* 30, 606–617. <https://doi.org/10.1016/j.apgeog.2010.01.005>

955 Singh, S.K., Srivastava, P.K., Gupta, M., Thakur, J.K., Mukherjee, S., 2014. Appraisal of land
956 use/land cover of mangrove forest ecosystem using support vector machine. *Environ.*
957 *Earth Sci.* 71, 2245–2255. <https://doi.org/10.1007/s12665-013-2628-0>

958 Sivakumar, M.V.K., 2007. Interactions between climate and desertification. *Agric. For.*
959 *Meteorol.* 142, 143–155. <https://doi.org/10.1016/j.agrformet.2006.03.025>

960 Sun, Q., Miao, C., Duan, Q., Ashouri, H., Sorooshian, S., Hsu, K.L., 2018. A Review of Global
961 Precipitation Data Sets: Data Sources, Estimation, and Intercomparisons. *Rev. Geophys.*
962 56, 79–107. <https://doi.org/10.1002/2017RG000574>

963 Symstad, A.J., Jonas, J.L., 2011. Incorporating biodiversity into rangeland health: Plant species
964 richness and diversity in great plains grasslands. *Rangel. Ecol. Manag.* 64, 555–572.
965 <https://doi.org/10.2111/REM-D-10-00136.1>

966 Turner, W., Spector, S., Gardiner, N., Fladeland, M., Sterling, E., Steininger, M., 2003. Remote
967 sensing for biodiversity science and conservation. *Trends Ecol. Evol.*
968 [https://doi.org/10.1016/S0169-5347\(03\)00070-3](https://doi.org/10.1016/S0169-5347(03)00070-3)

969 UNISDR, 2021. Inventar [WWW Document]. *Desaster Inf. Syst.* URL

970 <http://www.desinventar.lk:8081/DesInventar/> (accessed 5.14.21).

971 Vannoppen, W., Vanmaercke, M., De Baets, S., Poesen, J., 2015. A review of the mechanical
972 effects of plant roots on concentrated flow erosion rates. *Earth-Science Rev.*
973 <https://doi.org/10.1016/j.earscirev.2015.08.011>

974 Visser, S., Keesstra, S., Maas, G., de Cleen, M., Molenaar, C., 2019. Soil as a basis to create
975 enabling conditions for transitions towards sustainable land management as a key to
976 achieve the SDGs by 2030. *Sustain.* 11, 6792. <https://doi.org/10.3390/su11236792>

977 Wang, Z., Hou, Y., Fang, H., Yu, D., Zhang, M., Xu, C., Chen, M., Sun, L., 2012. Effects of
978 plant species diversity on soil conservation and stability in the secondary succession
979 phases of a semihumid evergreen broadleaf forest in China. *J. Soil Water Conserv.* 67,
980 311–320. <https://doi.org/10.2489/jswc.67.4.311>

981 Waring, R.H., Coops, N.C., Fan, W., Nightingale, J.M., 2006. MODIS enhanced vegetation
982 index predicts tree species richness across forested ecoregions in the contiguous U.S.A.
983 *Remote Sens. Environ.* 103, 218–226. <https://doi.org/10.1016/j.rse.2006.05.007>

984 Warren, S.D., Alt, M., Olson, K.D., Irl, S.D.H., Steinbauer, M.J., Jentsch, A., 2014. The
985 relationship between the spectral diversity of satellite imagery, habitat heterogeneity, and
986 plant species richness. *Ecol. Inform.* 24, 160–168.
987 <https://doi.org/10.1016/j.ecoinf.2014.08.006>

988 Wessels, K.J., Prince, S.D., Malherbe, J., Small, J., Frost, P.E., VanZyl, D., 2007. Can human-
989 induced land degradation be distinguished from the effects of rainfall variability? A case
990 study in South Africa. *J. Arid Environ.* 68, 271–297.
991 <https://doi.org/10.1016/j.jaridenv.2006.05.015>

992 Wessels, K.J., Prince, S.D., Reshef, I., 2008. Mapping land degradation by comparison of
993 vegetation production to spatially derived estimates of potential production. *J. Arid
994 Environ.* 72, 1940–1949. <https://doi.org/10.1016/j.jaridenv.2008.05.011>

995 Wessels, K.J., van den Bergh, F., Scholes, R.J., 2012. Limits to detectability of land
996 degradation by trend analysis of vegetation index data. *Remote Sens. Environ.* 125, 10–
997 22. <https://doi.org/10.1016/j.rse.2012.06.022>

998 Wickramagamage, P., 1998. Large-scale deforestation for plantation agriculture in the hill
999 country of Sri Lanka and its impacts. *Hydrol. Process.* 12, 2015–2028.
1000 [https://doi.org/10.1002/\(sici\)1099-1085\(19981030\)12:13/14<2015::aid-
1001 hyp716>3.0.co;2-3](https://doi.org/10.1002/(sici)1099-1085(19981030)12:13/14<2015::aid-

1001 hyp716>3.0.co;2-3)

1002 Yang, X., Zhang, M., Oliveira, L., Ollivier, Q.R., Faulkner, S., Roff, A., 2020. Rapid
1003 assessment of hillslope erosion risk after the 2019–2020 wildfires and storm events in

1004 sydney drinking water catchment. Remote Sens. 12, 1–20.
1005 <https://doi.org/10.3390/rs12223805>
1006 Yengoh, G.T., Dent, D., Olsson, L., Tengberg, A.E., Tucker, C.J., 2014. The use of the
1007 Normalized Difference Vegetation Index (NDVI) to assess land degradation at multiple
1008 scales: a review of the current status, future trends, and practical considerations,
1009 SpringerBriefs in Environmental Science. Springer International Publishing, Cham.
1010 <https://doi.org/10.1007/978-3-319-24112-8>
1011